

N eutralino D ark M atter, b- Yukawa Uni cation and N on-U niversal S ferm ion M asses

S. Profumo

Scuola Internazionale Superiore di Studi Avanzati (SISSA -ISA S), I-34014 Trieste, Italy
and Istituto Nazionale di Fisica Nucleare, Sezione di Trieste, I-34014 Trieste, Italy

Abstract

We study the implications of non-universal boundary conditions in the sfermion Soft SUSY Breaking (SSB) masses of M SUGRA. We impose asymptotic Yukawa coupling Unification and we resort to a parameterization of the deviation from Universality in the SSB motivated by the multiplet structure of SU(5) GUT. A set of cosmological constraints, including the recent results from WMAP, determines the allowed parameter space of the models under consideration. We highlight a "new coannihilation corridor" where \tilde{b}_1 and $\tilde{\chi}_1^0$ coannihilations significantly contribute to the reduction of the neutralino relic density.

Keywords: SUSY GUT models, Yukawa Unification, Non-Universality, Dark Matter, Coannihilations.

PACS numbers: 12.60.Jv, 12.10.Kt, 14.80.Ly, 95.35.+d

1 Introduction

The minimal supersymmetric extension of the Standard Model (MSSM) and Grand Unification are often regarded as the main ingredients of the physics beyond the Standard Model [1, 2, 3]. The phenomenological implications of the MSSM and of Grand Unification have been investigated since decades, and, though direct evidence of such theories is still missing, a large set of increasingly stringent constraints has put important bounds on the parameter space of these so-called SUSY-GUTs.

Nonetheless, the theoretical frameworks of SUSY-GUTs are countless, and typically characterized by a huge number of parameters. The common phenomenological practice is to make a certain number of (hopefully) theoretically motivated assumptions in order to deal with a reduced set of parameters. The first assumption one has to make in the context of SUSY is how to parameterize the mechanism of SUSY breaking.

Here, we resort to one of the most widely studied such contexts, the one of the so called supergravity models. In this framework, SUSY is broken in a hidden sector, whose fields couple only gravitationally to the MSSM fields [4]. Embedding the model in a GUT, and under some further assumptions (Gaugino and Scalar Universality), the soft SUSY breaking part of the Lagrangian of supergravity models is described by four continuous parameters plus one sign (m_{SUGRA}).

In this paper, based on the results presented in [5], we study a (minimal) deviation from Universality in the scalar fermions sector of the theory, inspired by the multiplet structure of the simplest GUT, $SU(5)$ (see Sec. 2.2). We apply to the model the constraint of b-Yukawa Coupling Unification, which is a common prediction of a wide set of Theories of Grand Unification, among which $SU(5)$ and $SO(10)$ GUTs.

One of the virtues of R-parity conserving SUSY models is to produce ideal candidates for cold dark matter, in the present case the lightest neutralino (a linear superposition of the neutral gauge and Higgs boson superpartners). The neutralino is, in fact, a color and electromagnetically neutral, weakly interacting massive particle (WIMP), as required to be a good cold dark matter candidate. The recent results from the WMAP satellite [6], combined with other astrophysical data, determined with unprecedented accuracy the Dark Matter content range of the Universe. It has been shown [7, 8] that the cosmologically allowed parameter space of m_{SUGRA} is dramatically restricted by the considerably lowered upper bound on the neutralino relic density. Moreover, as recently pointed out in Ref. [9], in cosmological scenarios involving quintessential fields, the relic density could undergo a further significant enhancement, even of several orders of magnitude. The necessity of efficient relic density suppression mechanisms is therefore by now an uncontroversial point.

One of the known mechanisms of neutralino relic density suppression occurs when the next-to-lightest supersymmetric particle (NLSP), is close in mass to the neutralino. In this case the neutralino relic density is not only suppressed by neutralino-neutralino annihilations, but also by coannihilations with the NLSP, and indirectly also by the annihilations of the NLSP itself [10, 11, 12].

This mechanism can involve in m_{SUGRA} various sparticles, such as the lightest stau [13, 14], stop [15], or chargino [16, 14]. In the present paper we address the possibility that minimal non-Universality in the sfermion sector can produce "new", unusual coan-

nihilation partners. We find that this possibility is effectively realized, in what we call a new coannihilation corridor, where the sbottom and the tau sneutrino play the role of NLSP. We show that this pattern is compatible with b-exact ("top-down") Yukawa Unification, and with all known phenomenological requirements.

In the next Section we introduce and motivate the model we analyze. We discuss the issue of b-YU and of a GUT-motivated minimal fermion SSB masses non-Universality. We then show in Sec.4 the features of the resulting particle spectrum, which gives rise to "new coannihilation corridors" involving, besides the stau, the lightest sbottom and the tau sneutrino. Sec.5 is devoted to the description of the cosmological phenomenological requirements we apply. We demonstrate in particular that the $b > 0$ case is not compatible with b- "top-down" YU. In Sec.6 we describe the new coannihilation regions. After our remarks, we give in the Appendix the complete list of the coannihilation processes involving neutralino, sbottom, tau sneutrino and stau. Finally, an approximate treatment of the neutralino relic density contributions coming from sbottom-sbottom, sbottom-neutralino and stau-tau sneutrino coannihilations is provided.

2 The Model

2.1 b-Yukawa Unification

One of the successful predictions of Grand Unified Theories is the asymptotic unification of the third family Yukawa couplings [1]. The issue of Yukawa Unification (YU) has been extensively studied, see e.g. [17, 18]. In particular, in this paper we address the YU of the bottom quark and of the tau lepton, which is a prediction of some of the minimal grand unification gauge group, such as SU(5). b-YU is a consequence of the fact that the two particles belong to the same SU(5) multiplet, and therefore, at the scale of grand unification M_{GUT} they are predicted to have the same Yukawa coupling. The experimental difference between m_b and m_τ is then mainly explained by two effects. First, the renormalization group running from M_{GUT} to the electroweak scale naturally drives the two masses to different values. Second, in the minimal supersymmetric standard model, the supersymmetric sparticles affect with different finite radiative corrections the values of the masses, in particular the one of the b quark [19].

Previous investigations of b-YU include Ref. [20] as regards non supersymmetric GUTs and Ref. [21, 22, 23, 18, 24], and more recently Ref. [26, 25] for the SUSY-GUT case. In particular, in [25] the implications of the recent experimental, and theoretical, results on the muon anomalous magnetic moment and on the inclusive branching ratio $b^+ \rightarrow e^+ \gamma$ were also taken into account, while in [27] the neutralino relic density constrain was examined, in the context of gaugino non-Universality. In Ref. [28, 29, 30] the puzzle of neutrino masses and mixing has been addressed in the context of b-YU.

A possible approach to b-YU is of the "bottom-up" type [24, 25]. It consists in defining some parameter which evaluates the accuracy of YU, such as

$$b = \frac{h_b(M_{\text{GUT}}) - h(M_{\text{GUT}})}{h(M_{\text{GUT}})} :$$

The procedure we take here is instead a "top-down" approach [26, 22, 23]: for a given set of SUSY parameters we fix the value $h(M_{\text{GUT}}) = h_b(M_{\text{GUT}})$ requiring the resulting m_b to be equal to its central experimental value. We then compute $m_b(M_Z)$ through RG running and taking into account the SUSY corrections. A model giving a value of the b-quark mass lying outside the experimental range is ruled out. With this procedure, we perform exact b-YU at the GUT scale, and directly check whether a given model can, or cannot, be compatible with it.

2.2 Minimal Sfermion Non-Universality

The parameter space of the minimal supersymmetric extension of the standard model (MSSM), in its most general form, includes more than a hundred parameters [31, 32]. Therefore, it is commonly assumed that some underlying principle reduces the number of parameters appearing in the Soft Supersymmetry Breaking (SSB) Lagrangian. In particular, in the case of gravity mediated supersymmetry breaking, one can theoretically motivate [4] the assumption that there exists, at some high energy scale M_x , a common mass m_0 for all scalars as well as a common trilinear term A_0 for all SSB trilinear interactions. Moreover, in SUSY GUT scenarios, the additional assumption that the vacuum expectation value of the gauge kinetic function does not break the unifying gauge symmetry yields a common mass $M_{1=2}$ for all gauginos. One is then left with four parameters ($m_0; A_0; M_{1=2}; \tan\beta$) and one sign (sign ϵ), which define the so-called constrained MSSM, or mSUGRA, parameter space.

Much work has been done in the investigation of non-Universality in the gaugino sector, see e.g. Ref. [33, 34]. As regards the SSB scalar masses, it has been since long known that Universality is not a consequence of the supergravity framework, but rather an additional assumption [35]. This justified an uprising interest in the possible consequences of non-Universality in the scalar sector [36, 37]. In particular, in [38] an analysis of various possible deviations from Universality in the SSB was carried out.

In this paper we focus on a simple model exhibiting minimal non-Universal sfermion masses (mNUSM) at the GUT scale. Our model is inspired by an SU(5) SUSY GUT where the scale of SSB Universality M_x is higher than the GUT scale M_{GUT} [38]. The RG evolution of the SSB from M_x down to M_{GUT} induces a pattern of non-Universality in the sfermion sector dictated by the arrangement of the matter fields into the supermultiplets:

$$\hat{L}; \hat{D}^c \quad ! \quad \bar{5} \quad (1)$$

$$\hat{Q}; \hat{U}^c; \hat{E}^c \quad ! \quad 10 \quad (2)$$

This structure entails the following pattern of sfermion mass non-Universality at the GUT scale:

$$m_L^2 = m_D^2 = m_5^2 \quad (3)$$

$$m_Q^2 = m_U^2 = m_E^2 = m_{10}^2 \quad (4)$$

The running between M_x and M_{GUT} will also produce two other effects. First, a typically large deviation from Universality and a splitting between the up and down Higgs masses

m_{H_1} and m_{H_2} is generated at the GUT scale (a detailed study of non-Universal Higgs masses is presented in [37] and [39]). Second, a small splitting is also present between the SSB masses of the two lightest sfermion families and the third one. In the present paper we will however restrict to a phenomenological parameterization of sfermion non-Universality, simply setting

$$m_{10}^2 = m_0^2 \quad (5)$$

$$m_5^2 = K^2 m_{10}^2 = K^2 m_0^2 \quad (6)$$

$$m_{H_1}^2 = m_{H_2}^2 = m_0^2 \quad (7)$$

We are therefore left with a single parameter K , which scans this "minimal", GUT-inspired deviation from Universality in the sfermion sector.

For our purposes, we let K vary between 0 and 1: in this way we recover full Universality (i.e. the CM SSM) for $K = 1$, while, for $K < 1$, we can lower the spectrum of the sparticles belonging to the $\bar{5}$ multiplet. Hence, we generate a spectrum with significantly lower masses for the tau sneutrino and the lightest stau and sbottom. Whenever the masses of these sparticles are close to the neutralino mass, they can play an important role in coannihilation processes.

3 Numerical Procedure

The minimal model we propose is defined by the following parameters:

$$m_0; A_0; M_{1=2}; \tan \beta; \text{sign } \mu \text{ and } K: \quad (8)$$

We impose gauge and b-Yukawa coupling Unification at a GUT scale M_{GUT} self-consistently determined by two-loops SUSY renormalization group equations [40] both for the gauge and for the Yukawa couplings between M_{GUT} and a common SUSY threshold M_{SUSY} , $\frac{P}{m_{\tilde{t}_1} m_{\tilde{t}_2}}$ ($\tilde{t}_{1,2}$ are the stop quark mass eigenvalues). At M_{SUSY} we require radiative electroweak symmetry breaking, we evaluate the SUSY spectrum and calculate the SUSY corrections to the b and t masses [23]. For the latter we use the approximate formula of Ref. [41]:

$$\frac{m_t}{m} = \frac{g_1^2}{16^2} \frac{M_2 \tan \beta}{M_2^2} (F(M_2; m_\infty) - F(0; m_\infty)); \quad (9)$$

$$F(m_1; m_2) = \ln \frac{M_2^2}{M_{\text{SUSY}}^2} + 1 + \frac{m^2}{m^2 - M^2} \ln \frac{M^2}{m^2}; \quad (10)$$

$$M = \max(m_1; m_2); m = \min(m_1; m_2); \quad (11)$$

From M_{SUSY} to M_Z the running is continued via the SM one-loop RGEs. We use fixed values for the running top quark mass $m_t(M_t) = 166$ GeV, for the running tau lepton mass $m_\tau(M_Z) = 1.746$ GeV and for $s(M_Z) = 0.1185$, fixed to its central experimental value. The asymptotic values of $h_b(M_{\text{GUT}}) = h_b(M_{\text{GUT}})$ and of $h_t(M_{\text{GUT}})$ are then consistently determined to get the central values of the top and tau masses, while the tree level m_b^{tree} and the SUSY-corrected m_b^{corr} masses of the running bottom quark at M_Z are outputs.

The neutralino relic density is computed interfacing the output of the RG E running with the publicly available code micrOMEGAs [42], which includes thermally averaged exact tree-level cross-sections of all possible (co-)annihilation processes, an appropriate treatment of poles and the one-loop QCD corrections to the Higgs coupling with the fermions. The output of micrOMEGAs also produces the relative contributions of any given final state to the reduction of the neutralino relic density.

The direct and indirect detection rates are estimated through another publicly available numerical code, darkSUSY [43].

As regards the phenomenological constraints, the Higgs boson masses are calculated using micrOMEGAs [42], which incorporates the FeynHiggsFast [44] code, where the SUSY contributions are calculated at two-loops. The inclusive BR ($b \bar{b} \rightarrow H \bar{H}$) is again calculated with the current updated version of the micrOMEGAs code [45], where the SM contributions are evaluated using the formalism of Ref. [46] and the charged Higgs boson SUSY contributions are computed including the next-to-leading order SUSY QCD resummed corrections and the $\tan\beta$ enhanced contributions (see Ref. [47]). The SUSY contributions to the muon anomalous magnetic moment a_μ are directly calculated from the formula of Ref. [48] and compared with the output of the micrOMEGAs code.

4 The Particle Spectrum with m NUSM

In minimal supergravity, especially after the very precise results from the WMAP satellite [6], giving a considerably reduced upper limit on the CDM density of the Universe, the cosmologically allowed regions of the parameter space are strongly constrained [7, 8]. As pointed out in [49, 50], mainly two mechanisms can suppress the neutralino relic density to sufficiently low values. The first one are coannihilations of the neutralino with the next-to-lightest sparticles (NLSP), which are effective whenever the mass of the latter lies within 10–20% of the neutralino mass [51, 10, 11]. The second mechanism is given by direct, rapid s-channel annihilation of the neutralino with the CP-odd Higgs boson A , which takes place if $m_A \neq 2m_\tilde{\chi}$, i.e. if the channel is enhanced by pole effects. In particular, we chose to focus here on the case of coannihilations, which in the present scenario of m NUSM are expected to exhibit a rich pattern.

In order to understand the possible pattern of coannihilations emerging from the parameterization of sfermion mass non-Universality outlined in Sec. 2.2, we study the spectrum of the candidate NLSPs, namely the lightest sbottom and the tau sneutrino. The dependence of the respective masses of these two sparticles on the high energy SSB inputs can be parameterized as follows:

$$m_{\tilde{b}_1}^2 = a_{\tilde{b}_1} K^2 m_0^2 + b_{\tilde{b}_1} m_0^2 + c_{\tilde{b}_1} M_{1=2}^2 + \dots \quad (12)$$

$$m_{\tilde{\tau}}^2 = a_{\tilde{\tau}} K^2 m_0^2 + b_{\tilde{\tau}} m_0^2 + c_{\tilde{\tau}} M_{1=2}^2 + \dots \quad (13)$$

¹Since here $m_A \neq m_H$, where H is the heaviest CP-even neutral Higgs boson, the condition $m_A \neq 2m_\tilde{\chi}$ implies pole effects also for H . However, the coupling of A to the dominant final states $b\bar{b}$ and $\tau^+\tau^-$ gets an enhancement factor, at large $\tan\beta$, equal to $(\tan\beta \cos\beta = \cos\beta)$ w.r.t. the coupling of H , whose contribution is therefore suppressed.

The contributions originate in part from the $SU(2)_L$ and $U(1)_Y$ D-term quartic interactions of the form $(\text{squark})^2 (\text{Higgs})^2$ and $(\text{slepton})^2 (\text{Higgs})^2$, and are $\propto \cos(2\beta) M_Z^2$ [2]. The sbottom mass gets a further contribution in \tilde{m}_b arising from the LR off-diagonal elements of the mass matrix. The mixing terms are generated by the typically large values of A_b , in its turn induced, even for $A_0(M_{\text{GUT}}) = 0$, by RG running, and by a $\tan\beta$ -enhanced contribution $\propto m_b$. In the case of the tau sneutrino, instead, a further, though small, contribution to \tilde{m}_τ analogously arises from A_τ .

We plot in Fig.1 (a) and (b) the typical behaviors of the sparticle masses as functions of K , at fixed $M_{1=2}$; m_0 and $\tan\beta$. Panel (a) shows the case of the mass of the sbottom, (we also plot the corresponding masses of the lightest neutralino and chargino). The high energy parameters are fixed at $M_{1=2} = 1100$ GeV, $\tan\beta = 38.0$, $A_0 = 0$ and $m_0 = 2850$; 3300 and 3750 GeV. We clearly see from the figure that the behavior is, as expected, $\tilde{m}_b \propto \frac{1}{K^2}$, where $\frac{1}{K^2} < 0$ is the sum of the terms in parenthesis in Eq.(12) and $\frac{1}{K^2} = a_{b_1} m_0^2 > 0$. Increasing the value of m_0 induces higher negative values for \tilde{m}_b , as well as obviously higher values for \tilde{m}_τ . We notice in any case that for sufficiently low values of K the mass of the sbottom is driven below the mass of the neutralino and also to negative values.

Panel (b) shows instead the mass of the tau sneutrino, at $M_{1=2} = 1100$ GeV, $\tan\beta = 38.0$, $A_0 = 0$ and $m_0 = 1350$; 1650 and 1950 GeV. We see that also here $\tilde{m}_\tau \propto \frac{1}{K^2}$, but in this case the interplay between b_1 and c_1 generates either positive ($m_0 = 1350$; 1650 GeV) or negative ($m_0 = 1950$ GeV). The outcome is therefore that the sneutrino mass can be lowered towards the mass of the neutralino for low values of K , depending on m_0 ; the typical range of m_0 for which this is possible is always lower than in the sbottom case.

We carried out a thorough investigation of the possible coannihilation regions, and we

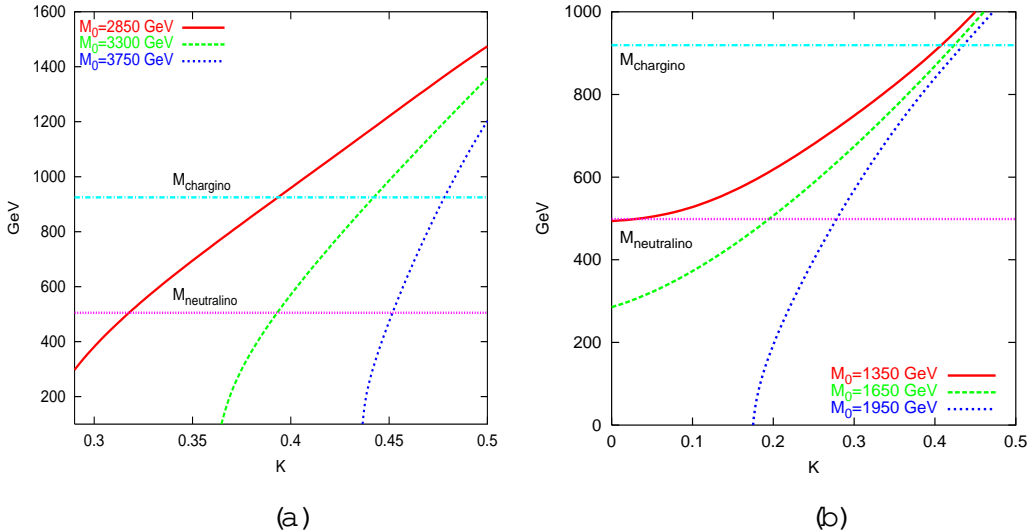


Figure 1: The sbottom (a) and sneutrino (b) spectrum at $M_{1=2} = 1.1$ TeV, $\tan\beta = 38.0$ and $A_0 = 0$ for different values of m_0 .

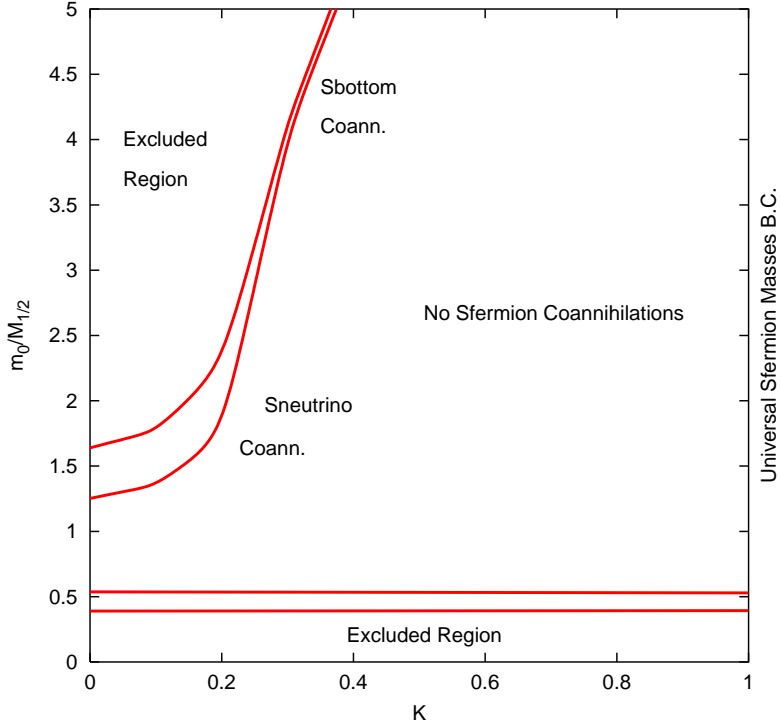


Figure 2: Coannihilation regions in the $(m_0 = M_{1=2}; K)$ plane at $M_{1=2} = 1.1$ TeV, $\tan \theta = 38.0$ and $A_0 = 0$. Points within the red lines are characterized by $\frac{m_{NLSP}}{m_{\tilde{\chi}}} \leq 20\%$. In the top left and lower part of the figure the LSP is not a neutralino, while in the top right region no coannihilations take place between the neutralino and the sleptons.

found that a good parameter is represented by the ratio $(m_0/M_{1=2})$ at fixed $\tan \theta$, $M_{1=2}$ and A_0 . In Fig 2 we plot the Coannihilation Corridors which we found scanning the plane $(m_0/M_{1=2}; K)$ at $M_{1=2} = 1.1$ TeV, $\tan \theta = 38.0$ and $A_0 = 0$. Within the red solid lines $\frac{m_{NLSP}}{m_{\tilde{\chi}}} \leq 20\%$. In the lower part of the figure, which we indicate as 'Excluded Region', the low value of m_0 implies that the stau becomes lighter than the neutralino, or even gets a negative (unphysical) mass. Very stringent bounds [52] indicate that the LSP has to be electrically and color neutral, and therefore this region is excluded. The strip above this excluded region represents a first coannihilation corridor, where the NLSP is the stau. We notice that this region survives up to $K = 1$, i.e. fully Universal boundary conditions. It actually represents a slice of the narrow band, in the $(m_0; M_{1=2})$ planes, which is cosmologically allowed thanks to neutralino-stau coannihilations (see e.g. Fig. 1 and 2 of Ref. [7]).

For values of $K < 0.5$ we find a second, distinct, branch where the mass of the NLSP lies within 20% of the LSP mass. In the lower part of the branch (in Fig 2 up to $m_0 = M_{1=2} = 3$) the NLSP turns out to be the tau sneutrino, with the lightest stau which is quasi-degenerate with it (say within few percent, see the discussion in Sec. 6.2). Increasing m_0 and moving to the upper part of the branch, the lightest sbottom becomes the NLSP, while the

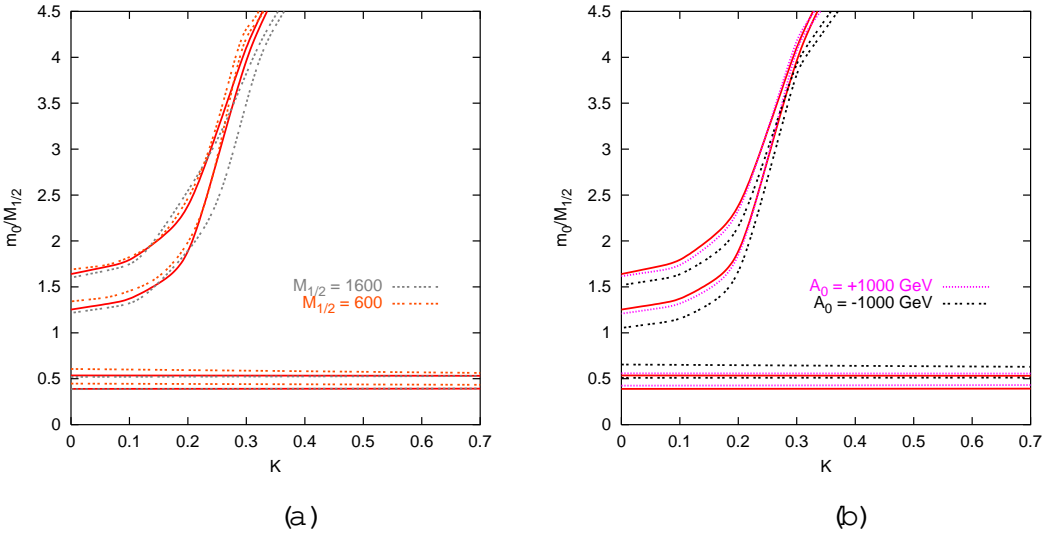


Figure 3: Coannihilation regions in the $(m_0/M_{1/2}; K)$ plane at $\tan\beta = 38.0$ and $A_0 = 0$. In Panel (a) the dependence on $M_{1/2}$ is studied at $A_0 = 0$. In Panel (b) two different values for the trilinear coupling $A_0 = \pm 1$ TeV are plotted at $M_{1/2} = 1100$ GeV.

tau sneutrino and the stau, still quasi degenerate among them, becomes by far heavier. In the upper left part of the figure, once again indicated as 'Excluded region', either the sbottom or the tau sneutrino become lighter than the neutralino, or even get negative values for their masses (see Fig.1). In Fig.3 we study the dependence of the shape of the coannihilation corridors on the various parameters which we fixed in Fig.2. In Panel (a) we vary the values of $M_{1/2}$, comparing the $M_{1/2} = 1100$ GeV case of Fig.2 with respectively $M_{1/2} = 1600$ GeV and $M_{1/2} = 600$ GeV. We see that there is practically no significant dependence of the shape on the value of $M_{1/2}$, and therefore we can conclude that the chosen parameter $m_0 = M_{1/2}$ is good, being $M_{1/2}$ -quasi independent. In Panel (b) we vary instead the value of the Universal trilinear coupling A_0 . We plot again with a red solid line the $A_0 = 0$ case, as well as the $A_0 = 1$ TeV and $A_0 = -1$ TeV cases, always at $\tan\beta = 38.0$ and $M_{1/2} = 1100$ GeV. Once again we do not see any significant effect, apart from a common shift of the lower coannihilation branch upwards and of the upper downwards. These shifts can be traced back to the effect of the off-diagonal A_0 (sign-independent) entries in the sfermion mass matrices.

Fig.4 illustrates the dependence on $\tan\beta$, highlighting this time a significant effect on the upper branch: increasing $\tan\beta$ yields higher values of K , i.e. the branch is moved to the right, and vice-versa. This effect can be qualitatively understood from the approximate expression for the mass eigenvalues of the relevant sfermions, Eq.(12), where an increase in $\tan\beta$ is compensated by an increase in the effective boundary value of the scalar masses, tuned by the parameter K . For instance, b_1 contains a negatively contributing term $/ \tan\beta m_b$, which is compensated, when the value of m_0 and of $m_{\tilde{b}}$ is fixed, by an increase of K .

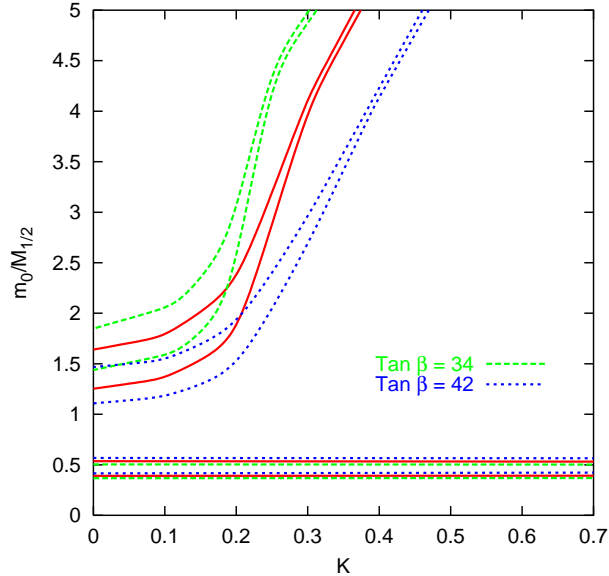


Figure 4: Coannihilation regions in the $(m_0/M_{1/2}; K)$ plane at $M_{1/2} = 1.1$ TeV and $A_0 = 0$. The red solid lines indicate the coannihilation corridor for $\tan \beta = 36.0$, while the green dashed and the blue dotted lines respectively $\tan \beta = 34; 42$.

5 Cosmological Phenomenological Bounds

In this paper we apply two classes of constraints: on the one hand the cosmological bounds coming from the limits on the cold dark matter content of the Universe and from direct and indirect neutralino searches; on the other hand we impose the most stringent "accelerator" constraints, such as the inclusive BR ($b \rightarrow s \gamma$) and the Higgs boson mass. In this second class we also include the bound on the b-quark mass, direct sparticle searches and a conservative approach [53] to the constraint coming from the SUSY corrections to the muon anomalous magnetic moment a_μ .

For illustrative purposes, we show the behavior of three Benchmark models, pertaining the three regions of coannihilations highlighted in the previous section. Namely, we choose three representative values of K and require the mass splitting between the neutralino and the NLSP to be 10%. We then scan the parameter space, setting $A_0 = 0$ and $\mu < 0$ for simplicity and varying m_0 . The features of the three models considered are summarized in Tab.1.

N LSP	m_{NLSP}	K	$\tan \beta$
stau	0.1	0.8	36.0
sbottom	0.1	0.4	36.0
tau sneutrino	0.1	0.2	36.0

Table 1: The three Benchmark scenarios described in the text

5.1 Neutralino Relic Density facing WMAP Results

Supersymmetric models with conserved R-parity generate ideal candidates for cold dark matter, as, in the present case, the neutralino. It is therefore natural to require, besides the fulfillment of the other phenomenological constraints, that the cosmological relic density of the neutralinos lies within the bounds indicated by cosmology. In particular, the recent results from the WMAP satellite [6], combined via a global fit procedure with other astrophysical data (including other CMB experiments, LSS surveys and the Lyman data), give a compelling bound on the cosmological relic density of Cold Dark Matter

$$h_{\text{CDM}}^2 = 0.1126^{+0.00805}_{-0.00905} \quad (14)$$

We take here the 2- range, and we require that $\sim h^2 \approx 0.1287$. Strictly speaking, the lower bound cannot be directly imposed, if we suppose that the neutralinos are not the only contributors to the cold dark matter of the Universe. For illustrative purposes, in Fig.11 we will plot also the lower bound on the relic density.

In Fig.5 we show instead the behavior of the neutralino relic density as a function of $m_{\tilde{A}}$ for the three Benchmark models. We see that in the case of tau sneutrino the coannihilations only weakly contribute to the reduction of the relic density (see Sec.6.2), which, as expected, quadratically diverges with $m_{\tilde{A}}$. In the case of the sbottom coannihilation, SUSY QCD effectively enhance the relic density suppression, which nonetheless still exhibits a divergent behavior. In the case of the stau, instead, we can see how the interplay between coannihilation and direct rapid annihilation through the A-pole s-channel can drastically reduce the relic density. In the dip located between 600 and 700 GeV, in fact, the splitting between the mass of the CP-odd Higgs boson and twice the mass of the neutralino $\frac{m_A}{2m_{\tilde{A}}}$ $\approx 3\%$, and therefore direct pole annihilations are extremely efficient, leading to viable values of $\sim h^2$ for rather high $m_{\tilde{A}} \approx 700$ GeV.

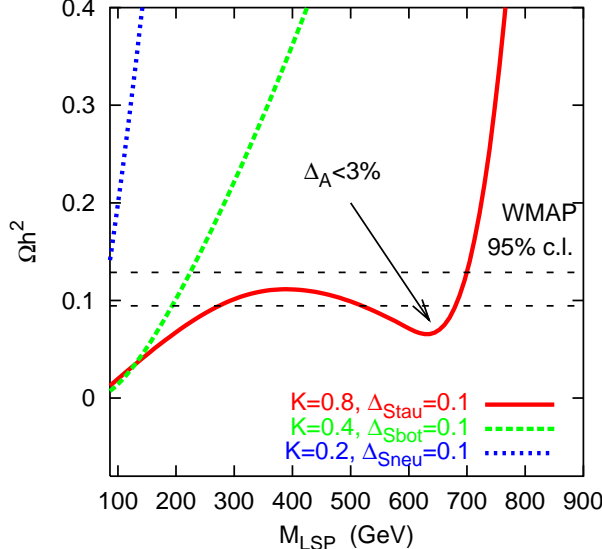


Figure 5: Neutralino Relic Density for the three Benchmark scenarios of Tab.1. The upper and lower bounds on h_{CDM}^2 are the 95% CL from WMAP global fit [6].

5.2 Direct and Indirect $W \bar{W}$ and $W \bar{W} \gamma$ searches

As pointed out in [34], non-Universality in the sfermion sector should not give rise to substantial modifications to $\sim_q^{\text{scalar; spin}}$. In fact, owing to the small Yukawa couplings of the lightest generation of quarks, NUSM do not greatly affect the masses of the up and down squarks, leading to substantially unchanged values for the direct annihilation cross sections, sensitive to processes like $\sim_q^{\text{scalar; spin}}$. As far as indirect detection (e.g. the muon flux from the Sun) is concerned, for the same reason non-Universality do not significantly affect the detection rates. We find in fact both for direct and indirect $W \bar{W}$ and $W \bar{W} \gamma$ searches, that NUSM produce detection rates in the same range of the CM SSM [54].

5.3 SUSY Corrections to the b-quark Mass

It has been already pointed out, see e.g. [25, 26], that the requirement of b^- Yukawa Unification favors negative values of \tilde{m}_b . We recall that \tilde{m}_b is one of the parameters included both in the CM SSM and in our NUSM model. In this section we demonstrate that, even with NUSM, $\tilde{m}_b > 0$ is not compatible with YU, and discuss the $\tilde{m}_b < 0$ which, instead, allows, in a suitable range the fulfillment of b^- YU.

The main problem of b^- YU with $\tilde{m}_b > 0$ is that one typically obtains a tree level mass for the b quark which is close to the experimental upper bound, and has to add on top of it large positive SUSY corrections (Eq.(16)), which drive m_b^{corr} outside the experimental range (or, the other way round, m_b far away from m_h). We impose b^- YU at the GUT scale, we fix $m_h(M_{\text{GUT}}) = h_b(M_{\text{GUT}})$ bottom-up from the properly corrected and RG evolved $m_b(M_z)$, obtaining as outputs the tree level m_b^{tree} and the SUSY-corrected m_b^{corr} masses of the running bottom quark at M_z . We compare these numbers with the appropriately evolved b-quark pole mass [56] up to the M_z scale, with $m_b(M_z) = 0.1185$, following the procedure of Ref. [57]:

$$m_b(m_b) = 4.25 \quad 0.3 \text{ GeV} \quad) \quad m_b(M_z) = 2.88 \quad 0.2 \text{ GeV} \quad (15)$$

The largest SUSY corrections arise from sbottom-gluino and stop-chargino loops, frozen at the M_{SUSY} scale [19, 41, 58]. They are non-decoupling effects because one gets a finite contribution even in the infinite sparticle mass limit, and they can be cast in the following approximate form :

$$\frac{m_b^g}{m_b} = \frac{2}{3} \frac{m_b^2}{M_3} I(m_{b_1}^2; m_{b_2}^2; M_3^2) \tan \beta; \quad (16)$$

$$\frac{m_b^{\tilde{m}}}{m_b} = \frac{Y_t^2}{16 \pi^2} A_t I(m_{t_1}^2; m_{t_2}^2; \tilde{m}_b^2) \tan \beta; \quad (17)$$

$$I(x; y; z) = \frac{xy \ln(x=y) + xz \ln(z=x) + yz \ln(y=z)}{(x-y)(y-z)(x-z)}; \quad (18)$$

Unless the trilinear coupling A_t is very large, the gluino loop typically dominate (an exception is investigated in Ref. [59]) and the sign of the SUSY contribution is given by

²We use here the standard sign conventions of Ref. [55]

the sign of M_3 . Therefore, since we assume here gaugino Universality, this implies that b^- YU is favored in the $\mu < 0$ case.

To numerically quantify this statement, we study the behavior of m_b^{tree} and m_b^{corr} varying the parameters of the mNUSM model. In Fig 6 (a) we fix $A_0 = 0$, $\tan\beta = 38.0$, $m_0 = 1000$ GeV and $M_{1/2} = 1100$ GeV, and analyze the dependence on K . We see that the tree level value m_b^{tree} is roughly constant, while the SUSY corrections decrease as K increases. Both remain however well above the experimental upper bound. This can be understood from Eq. (16), since increasing K means increasing $m_{\tilde{b}_1}$, with a fixed value for M_3 and, roughly, for $m_{\tilde{b}_2}$, and the function $I(x;y;z)$, at fixed y and z is inversely proportional to its other two arguments. Therefore, subsequently, we concentrate on the Universal $K = 1$ case, in order to check whether a parameter space allowing for "top-down" b^- YU exists or not.

The second step is to study the dependence of the b-quark mass on the parameter m_0 (Fig 6 (b)). We take here $A_0 = 0$, $\tan\beta = 38.0$; $M_{1/2} = 1100$ GeV and $K = 1$, and we notice, as expected, that the size of the corrections decreases with increasing m_0 . This is explained on the one hand by the fact that from the radiative EW SB condition the value of μ^2 is slightly decreased by the increase of m_0 [2], and on the other hand because increasing the value of $m_{\tilde{b}_{1,2}}$ leads to a decrease of the function I . In Fig.6 (c) we take instead $A_0 = 0$, $\tan\beta = 38.0$; $m_0 = 2000$ GeV and $K = 1$, and vary $M_{1/2}$. As can be easily inferred from Eq. (16), increasing $M_{1/2}$ leads to an increase both in M_3 and in μ . In conclusion, the candidate parameter space for b^- YU for $\mu > 0$ is at low $M_{1/2}$ and

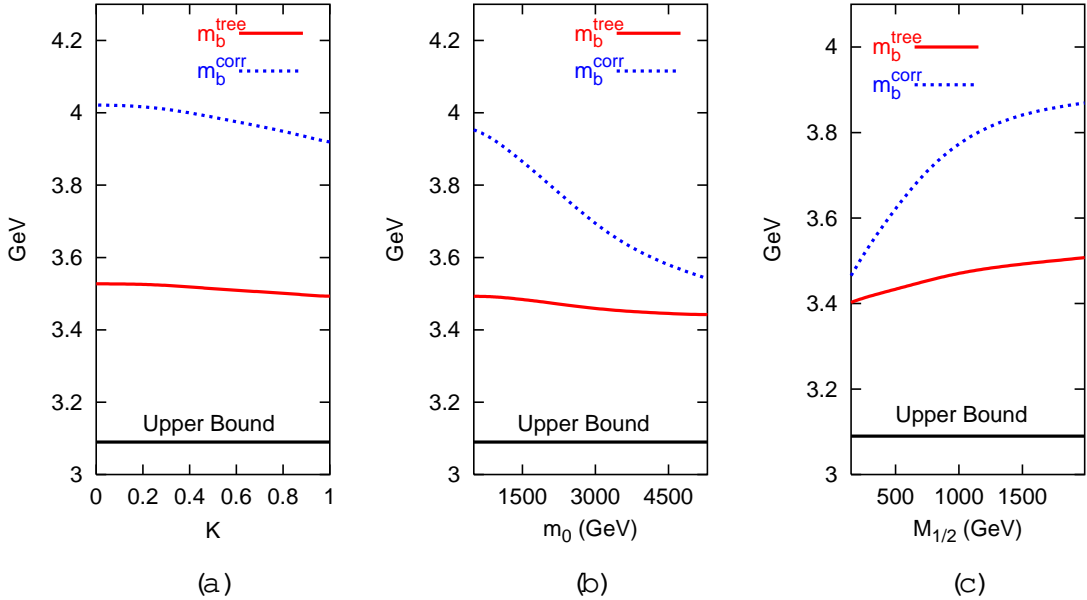


Figure 6: Tree level and SUSY corrected values of the b-quark mass at $\tan\beta = 38.0$ and $A_0 = 0$. In Panel (a) the parameter K is varied at fixed $M_{1/2} = 1100$ GeV and $m_0 = 1000$ GeV. In Panel (b) m_0 is varied at fixed $M_{1/2} = 1100$ GeV and $K = 1$. Finally, in Panel (c) the dependence on $M_{1/2}$ is studied at $m_0 = 2000$ GeV and $K = 1$.

high m_0 values. We choose therefore two trial values, $M_{1=2} = 300$ GeV; $m_0 = 2000$ GeV and we show our results in Fig.7. As readily seen from Eq. (16), we find that the SUSY contributions grow with $\tan\beta$. We notice however that the tree level mass strongly decreases with $\tan\beta$, owing to the fact that the positive SUSY contributions to m_b (see Eq. (9)) imply a smaller value for the asymptotic common b -Yukawa coupling. The overall conspiracy of these two effects is to maintain the corrected b quark mass well above the experimental upper bound. This conclusion is further confirmed investigating extreme values of $(M_{1=2}; m_0)$ for high $\tan\beta$, always in the Universal $K = 1$ case, and resorting also to nonzero values of A_0 .

To sum up, we demonstrated that, owing to the SUSY corrections to the b -quark mass, top-down b -YU is excluded, both with Universal and with minimal Non-Universal sfermion masses, in the case $\beta > 0$.

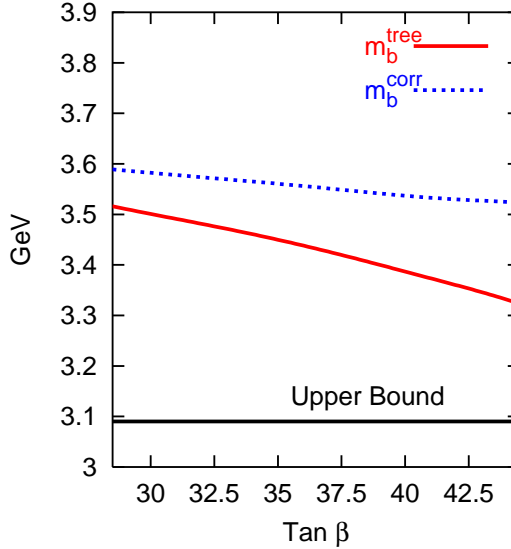


Figure 7: Tree level and SUSY corrected values of the b -quark mass at $M_{1=2} = 300$ GeV; $m_0 = 2000$ GeV; $A_0 = 0$ and $K = 1$.

5.3.1 The $\beta < 0$ Case

In the $\beta < 0$ case the SUSY contributions to the b -quark mass are negative, and therefore conspire to bring the tree level mass dictated by b -YU within the experimental range (15). We plot in Fig.8 (a) the tree level and SUSY-corrected values of the b -quark mass for the three Benchmark models of Tab.1. We notice that the size of the SUSY corrections decrease when m_0 is increased, because of the mentioned behavior of the function $I(x; y; z)$ of Eq.(16), which is inverse-proportional to its arguments. In the case of the sbottom coannihilation (green dashed line) the effect is enhanced by the large size of m_0 which, through the reduction of β due to the EW SB condition, directly reduces the size of the SUSY contributions.

5.4 The Inclusive B branching Ratio $b \rightarrow s$

We construct the 95% C.L. range on the BR ($b \rightarrow s$) starting from the recent experimental data of Ref. [60] and properly combining the experimental and theoretical uncertainties. The resulting bound is

$$1.9 \cdot 10^{-4} \leq \text{BR} (b \rightarrow s) \leq 4.6 \cdot 10^{-4} \quad (19)$$

We calculate the BR ($b \rightarrow s$) using the current updated version of micrOMEGAs [45]. The SM contribution is calculated through the formula of Ref. [46], while the SUSY corrections through the ones of Ref. [47]. We can estimate the dependence of the SUSY corrections from the approximate formula of Ref. [61, 62]. They are given, respectively for the charged Higgs and for the chargino exchanges, by

$$C^{H^+} = \frac{1}{2} \frac{m_t^2}{m_{H^+}^2} f^{H^+} - \frac{m_t^2}{m_{H^+}^2} \quad ; \quad (20)$$

$$C^{\tilde{c}} = (\text{sign } A_t) \frac{\tan \frac{m_t}{2}}{4} f^{\tilde{c}} - \frac{m_t^2}{2} f^{\tilde{c}} - \frac{m_t^2}{2} \quad ; \quad (21)$$

where

$$f^{H^+}(x) = \frac{3}{6(x-1)^2} + \frac{3x-2}{3(x-1)^3} \ln x; \quad (22)$$

$$f^{\tilde{c}}(x) = \frac{7x-5}{6(x-1)^2} - \frac{x(3x-2)}{3(x-1)^3} \ln x; \quad (23)$$

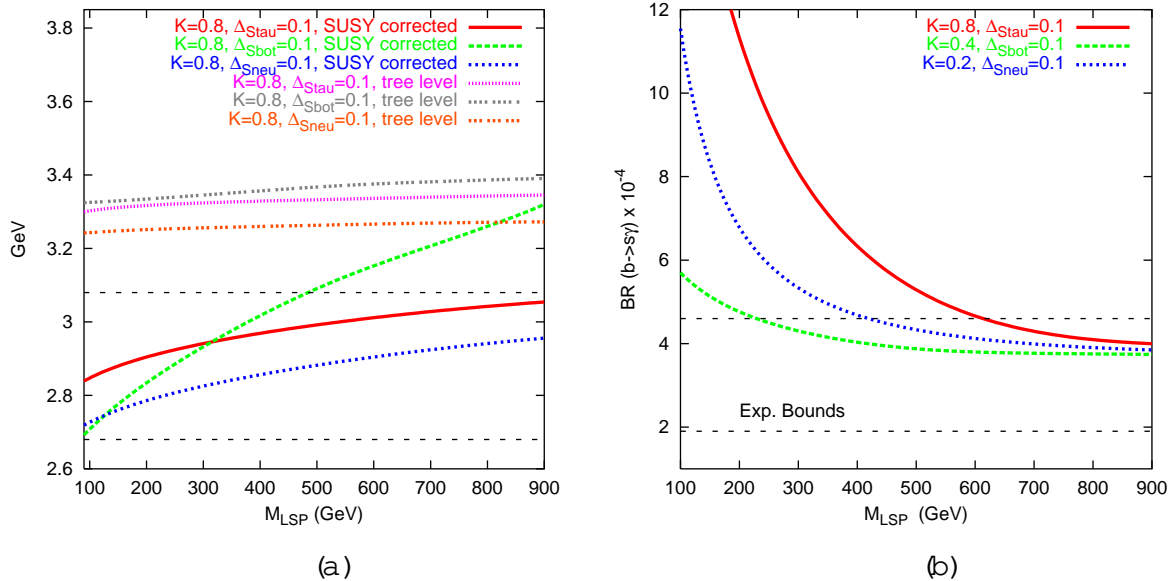


Figure 8: Tree level and SUSY corrected b-quark masses (a) and the BR ($b \rightarrow s$) for the three Benchmark scenarios of Tab.1. The upper and lower bounds are those of Eq. (15) for Panel (a) and those of Eq. (19) for Panel (b).

We notice that the relative sign of the two contributions of Eq. (20) and (21) is given by $\text{sign}(A_t) = \text{sign}(M_3)$, (the latter equality being valid for large top and bottom Yukawa couplings, as in the present case). Moreover, the SM contribution has the same sign as the charged Higgs one. All the contributions decrease as m_\sim increases, therefore we expect to draw a lower bound on the m_\sim from the lower bound on $\text{BR}(b \rightarrow s \gamma)$ (19) in the case $M_3 > 0$ and from the upper bound of Eq. (19) for $M_3 < 0$, which is the present case. We notice that the lower bound on m_\sim becomes more restrictive as $\tan \beta$ is increased, as can be read out from Eq. (21).

In Fig.8 (b) we plot the results we get for the three Benchmark scenarios of Tab.1. We can see that as the SUSY spectrum becomes heavier (we recall that if the sbottom is the NLSP $m_0 = M_{1=2} \approx 3$, see Fig.2) the lower bound on m_\sim weakens, as can be understood from Eq. (20) and (21) and from the explicit form of f^{H^+} and $f^{\tilde{H}}$.

5.5 The Higgs Bosons Masses

We take in our analysis the 95% C.L. LEP bound [63] on the lightest CP-even neutral Higgs boson mass

$$m_h \approx 114.3 \text{ GeV}; \quad (24)$$

which gives a lower bound on the m_\sim . Two loop corrections are taken into account, as described in Sec.3. In Fig.9 (a) we plot the results for the Higgs mass we obtain for the three Benchmark scenarios.

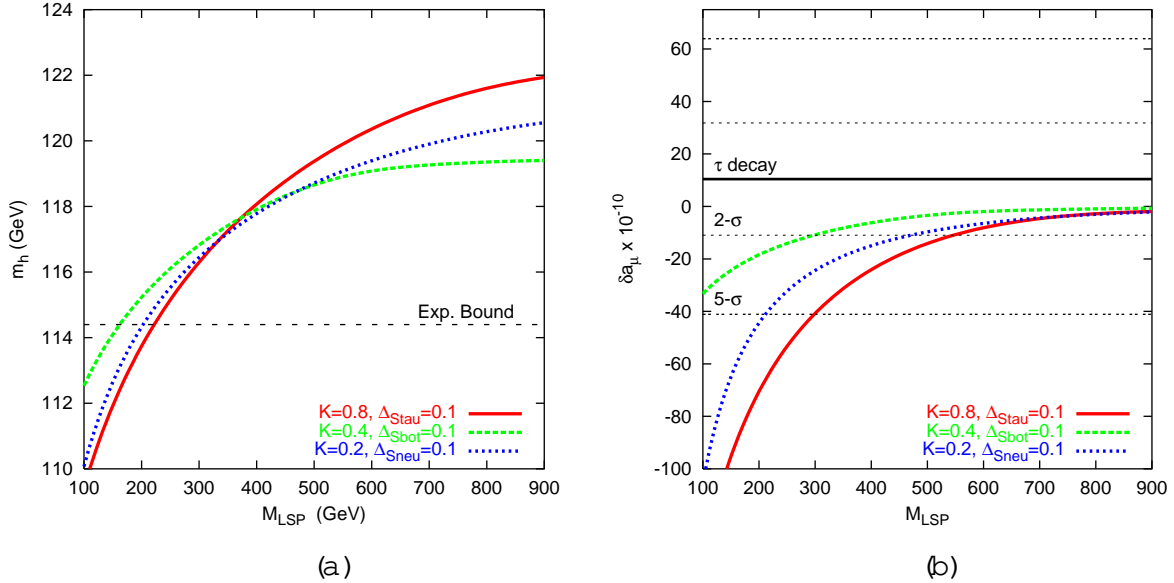


Figure 9: m_h (a) and $\delta a_\mu^{\text{SUSY}}$ (b) for the three Benchmark scenarios of Tab.1. The lower bound of Panel (a) is given in Eq. (24), while in Panel (b) the 2- and 5- σ bounds are taken from Eq. (27).

5.6 Direct Accelerators Sparticle Searches

We impose the current direct accelerator search limits on the sparticle masses [64], respectively $m_{\tilde{t}_1} > 104$ GeV, $m_{\tilde{b}_1} > 100$ GeV for $f = \tilde{t}_1, \tilde{b}_1, \tilde{t}_2, \tilde{b}_2$, $m_{\tilde{g}} > 300$ GeV, $m_{\tilde{\chi}_{1,2}} > 260$ GeV for $\tilde{q} = \tilde{u}, \tilde{d}, \tilde{s}, \tilde{c}$. We always find the constraints from BR (b → s) and from m_h more restrictive than the direct sparticle searches. Therefore we do not plot these bounds in the panels of Sec. 6.1 and 6.2.

5.7 The Muon Anomalous Magnetic Moment

The deviation a of the muon anomalous magnetic moment a from its predicted value in the Standard Model can be interpreted as arising from SUSY contributions, a^{SUSY} , given by neutralino-muon (a) and chargino-sneutrino (b) loops (See Fig. 10). The quantity a^{SUSY} , which we numerically compute with the micrOMEGAs package, can be estimated through the formula of Ref. [48], assuming a common value for the SUSY sparticles m_{SUSY}

$$a^{\text{SUSY}} = \text{sign}(M_2) \frac{\tan \theta_W}{192^2 m_{\text{SUSY}}^2} \frac{m^2}{(5g_2^2 + g_1^2)} : \quad (25)$$

On the experimental side, the BNL E821 experiment recently delivered a high precision measurement (0.7 ppm) of $a^{\text{exp}} = 11659203(8) \times 10^{-10}$. The theoretical computation of the SM prediction is plagued by the problem of estimating the hadronic vacuum polarization contribution. In particular, there is a persisting discrepancy between the calculations based on the decay data and those based on low-energy $e^+ e^-$ data. Recent evaluations [65, 66] give the following range for the deviation of the SM value of a from the experimental one:

$$a^{\text{exp}} - a^{\text{SM}} = (35.6 \pm 11.7) \times 10^{-10} \quad (e^+ e^-) \quad (26)$$

$$a^{\text{exp}} - a^{\text{SM}} = (10.4 \pm 10.7) \times 10^{-10} \quad (\text{decay}) \quad (27)$$

Following the lines of Ref [53] we decided to take a conservative approach to the problem of choosing which bound should be culled from the tantalizing results of Eq. (26, 27). In what follows we will therefore just indicate the region determined by the 2- and 5- range for the $e^+ e^-$ based approach and for the decay based approach, but we will not use this constraint to derive (lower) bounds on $m_{\tilde{\chi}_i}$.

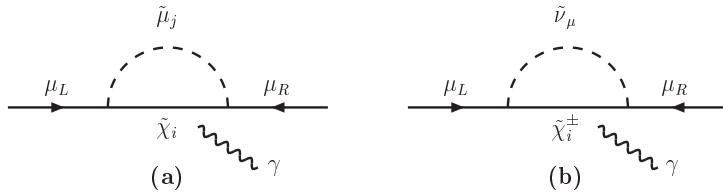


Figure 10: The main SUSY contributions to the muon anomalous magnetic moment: (a) neutralino-muon and (b) chargino-sneutrino loops.

In Fig.9 (b), where we present the results we get for the three Benchmark scenarios, we indicate only the decay based limit, since α_{SUSY}^{SUSY} , being < 0 , is negative (see Eq.(25)). Formula (25) allows us to interpret the results we show in Fig.9 (b) and in the Figures of the next Section. First, we see that as the SUSY spectrum becomes heavier (bottom NLSP case) the corrections become smaller, as emerging from (25). Second, we can see that α_{SUSY}^{SUSY} decreases with increasing $m_{\tilde{\chi}}$, for the same region as above, and that it increases with $\tan\beta$.

6 The "New" Coannihilation Corridor

In the $\beta < 0$ case the SUSY corrections to the b-quark mass are negative, and therefore can naturally drive the corrected $m_b^{\text{corr}}(M_Z)$ within the experimental range. From Eq. (16) we notice that the size of the corrections (linearly) grow with $\tan\beta$, therefore we expect that the upper bound on $m_b(M_Z)$ determine the lower bound on $\tan\beta$ and vice-versa. As will emerge clearly from the figures of Sec.6.1 and 6.2, the m_b constraint interplays with other cosmological bounds, and thus entails the determination of the allowed range of $\tan\beta$. In particular, we pin down the lowest limit on $\tan\beta$ combining the most restrictive phenomenological constraint, which turns out to be the BR(b → s̄) and which gives the lower bound on $m_{\tilde{\chi}}^{\text{min}} = m_{\tilde{\chi}}$, with the upper bound on m_b^{corr} , which in its turn gives the upper bound $m_{\tilde{\chi}}^{\text{max}}$. Requiring $m_{\tilde{\chi}}^{\text{min}} = m_{\tilde{\chi}}^{\text{max}}$ unambiguously gives the lowest allowed value of $\tan\beta$. In order to find the upper limit on $\tan\beta$, we notice that the bound on m_b is weaker than the constraint coming from BR(b → s̄) in determining the lowest value $m_{\tilde{\chi}}^{\text{min}}$ (see e.g. Fig.12 (b) and Fig.15 (b)). In fact, the BR(b → s̄) constraint becomes more and more stringent as one increases $\tan\beta$. On the other hand, $m_{\tilde{\chi}}^{\text{max}}$ is this time fixed by the cosmological constraint on the maximum allowed neutralino relic density (see Sec.5.1 and Fig.12 (b) and 15 (b)). Eventually, we find that in the $\beta < 0$ case the allowed $\tan\beta$ range is³

$$31^\circ \leq \tan\beta \leq 45^\circ \quad \beta < 0: \quad (28)$$

We checked that the range given in (28) is valid also at $A_0 \neq 0$. We find in fact that in this case an analogous procedure of determination of $(\tan\beta)^{\text{max}}, (\tan\beta)^{\text{min}}$ yields weaker limits. What happens at $A_0 \neq 0$ is mainly that the phenomenological bounds tend to push $m_{\tilde{\chi}}^{\text{min}}, m_{\tilde{\chi}}^{\text{max}}$ to higher values, therefore $(\tan\beta)^{\text{max}}$ is lowered, while $(\tan\beta)^{\text{min}}$ is left substantially unchanged.

6.1 $\tilde{b}_1 \sim \tilde{b}_1$ Coannihilations

As pointed out in Sec.4, the boundary conditions given by mNUSM produce a new "Coannihilation Branch", extending from $K = 0$ up to $K = 0.5$ and for values of m_0 greater

³As regards the A-pole region funnel, we obtained different, and typically wider, ranges for $m_{\tilde{\chi}}$. Since this region is not at all affected by fermion masses non-universality, as it depends only on the Higgs and on the neutralino masses, we do not give here the details of this determination. However, the EW SB condition, together with the other cosmological bounds, constrains the $\tan\beta$ range within the limits given in (28).

than $dM_{1=2}$, with c of $o(1)$, increasing with decreasing values of $\tan \alpha$. In the upper part of the branch, typically for $m_0 = M_{1=2} \approx 3$, the NLSP turns out to be the lightest sbottom. Being a strong-interacting particle, we find that its annihilation and coannihilations channels are very efficient, and substantially contribute to the neutralino relic density suppression.

We plot in Fig.11 and 12 (a) and (b) the cosmologically allowed regions for three representative values of $\tan \alpha = 34, 38$ and 42 for a fixed value of $K = 0.35$. The y axis represents the relative percent splitting between the neutralino mass and the next-to-lightest SUSY particle, in this case the lightest sbottom :

$$m_{NLSP} = \frac{m_{NLSP} - m_{\tilde{\chi}}}{m_{\tilde{\chi}}} : \quad (29)$$

The relevant phenomenological constraints described in the previous sections determine lower, and sometimes upper, limits on $m_{\tilde{\chi}}$. They are drawn as almost vertical lines, since they typically weakly depend on m_0 , which moreover very little varies in the plotted regions. They are instead fixed by $M_{1=2}$ (and therefore, in the plots, by $m_{\tilde{\chi}}$). The regions allowed by a given constraint lies at the right of the respective lines. Points below the red lines are characterized by relic densities which fall within the 2σ range of Eq. (14). In Fig.11 we also plot with a magenta dotted line the lower bound on $m_{\tilde{\chi}} h^2$. We see that the most stringent bound, for $\tan \alpha = 38.0$, is provided by the $BR(b \rightarrow s \gamma)$, while for higher values of $\tan \alpha$ the b-quark mass constraint becomes more restrictive. As far as the upper bound on $m_{\tilde{\chi}}$ is concerned, we find that high values of $\tan \alpha$ allow $m_{\tilde{\chi}}$ to extend

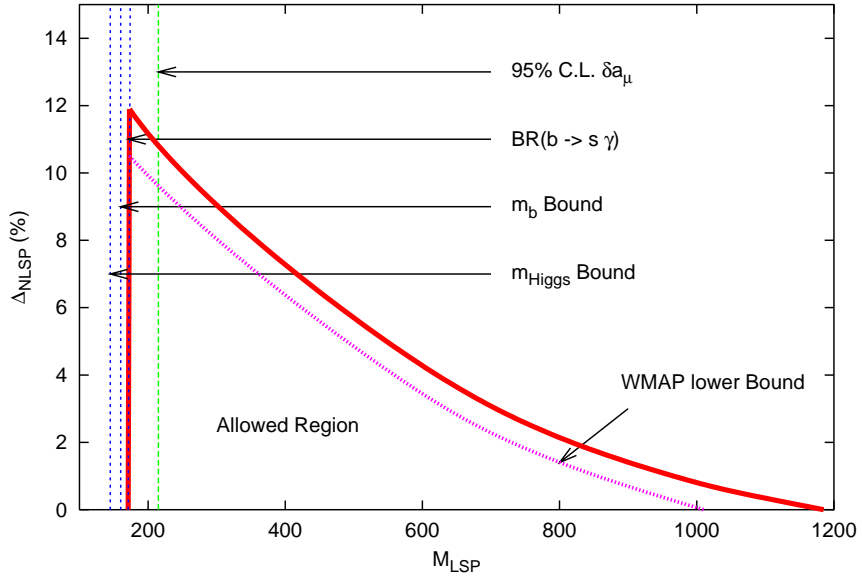


Figure 11: Cosmologically allowed parameter space in the sbottom coannihilation region, at $K = 0.35$ and $\tan \alpha = 38.0$. The region below the red solid line has $m_{\tilde{\chi}} h^2 < 0.1287$. The magenta line shows the putative lower bound on the neutralino relic density (14). The blue dotted nearly vertical lines indicate the phenomenological constraints described in the text, while the green dashed line stands for the 2σ bound on the muon anomalous magnetic moment.

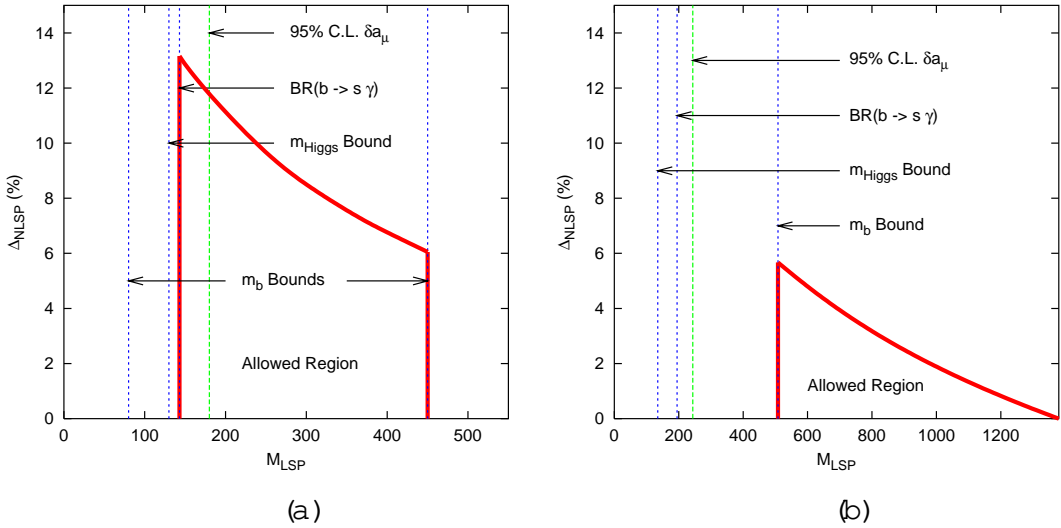


Figure 12: Cosmologically allowed parameter space in the sbottom coannihilation region at $K = 0.35$, $\tan \beta = 34.0$ (a) and $\tan \beta = 42.0$ (b).

up to 1.5 TeV (Fig.12 (b)). For smaller $\tan \beta$ the upper bound on $m_{\tilde{b}}$ is instead fixed by the upper bound on the b-quark mass: the SUSY corrections to m_b (see Eq.(9)) drive the common b-Yukawa coupling to higher values, therefore generating a higher tree level b-quark mass which is not compensated by the (smaller) negative SUSY corrections to m_b (Eq. (16)). The inverse mechanism pushes the lower bound on $m_{\tilde{b}}$ to higher values (0.5 TeV) in the case of $\tan \beta = 42$. We notice that the region determined by the 2-sigma range from the decay approach always covers the great part (or the totality) of the allowed parameter space.

In Fig.13 we studied the sensitivity of our results to a non-zero value of the common trilinear coupling A_0 at the GUT scale, for $\tan \beta = 38.0$, $b_1 \neq 0$ and $K = 0.35$. We notice that the lower limit on $m_{\tilde{b}}$ is fixed by the $A_0 = 0$ case. As for the cosmological bound on Δh^2 , the variation of A_0 leads to very little modifications of the upper bounds on $m_{\tilde{b}}$ displayed in Fig.11 and 12: we therefore conclude that the only relevant change is the type of constraint that, depending on the sign and on the absolute value of A_0 determines the lower bound on $m_{\tilde{b}}$.

As far as the coannihilation channels are concerned, the case of the sbottom is characterized by a rather simple pattern, clearly dominated by strong interaction processes. We find that for sbottom masses quasi-degenerate with the neutralino mass, the neutralino pair annihilation rate is very low (less than few percent). The dominant channels concern instead neutralino-sbottom coannihilations into gluon-b quark (up to 10%) and sbottom-sbottom annihilations into a couple of b quarks (up to 15%) or into a couple of gluons (up to 80%). We give in the Appendix (Sec. A.2) an approximate analytical treatment of these three most relevant processes.

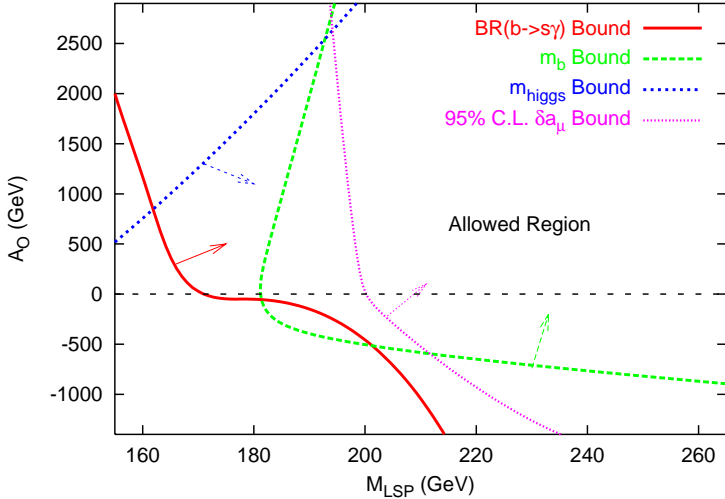


Figure 13: The determination of the lower bound on $m_{\tilde{\chi}}$ in the case of non zero A_0 , for $\tan\beta = 38.0$, $b_1 = 0$ and $K = 0.35$. The allowed region is in the upper right part of the figure, as indicated.

6.2 $\tilde{\chi}_1^0$ ~ Coannihilations

In the lower part of the new coannihilation branch of Fig 2, for $(m_0 = M_{1=2})$. 3 and $0 < K < 0.25$, the NLSP switches from the sbottom to the tau sneutrino. In this region the lightest stau is always heavier than the sneutrino, but the relative mass splitting is within few percent. This small splitting results from the combination of two RG effects:

$$m_{\tilde{\chi}}^2 = m_{\tilde{\chi}_1^0}^2 + \tilde{\chi}_{\text{LR}}(A) - c_1 \cos(2\beta) M_Z^2 : \quad (30)$$

The first contribution in Eq.(30) comes from the mixing between $\tilde{\chi}_L$ and $\tilde{\chi}_R$, which depends on A , while the second term stems from the mentioned D-term quartic interaction, and the coefficient $c_1 \approx 0.8$ [2]. Even though $A_0 = 0$ at the GUT scale, RG effects can drive A (M_{susy}) to large values (for the case of Fig 2 we obtain typical values for $A \approx 0.5$ TeV) and thus entail a non trivial LR mixing $\tilde{\chi}_{\text{LR}}$. In the case of Fig 2 we get $m_{\tilde{\chi}}^2 = m_{\tilde{\chi}_1^0}^2 \approx 10$ GeV.

In Fig.14 we plot the cosmologically allowed region at $K = 0.1$ and $\tan\beta = 38.0$, in analogy with Fig.11. We also show the "super-conservative" 5- σ bound on a , while the m_b bounds lie outside the depicted range.

Fig.11 and 14 allow to compare the efficiency of coannihilation processes involving a strongly interacting sparticle (the sbottom) and a weakly, or electromagnetically interacting one (the tau sneutrino and the stau). We see that in the second case the maximum mass splitting between the NLSP and the neutralino is 2%, while in the first one, at the same $m_{\tilde{\chi}}$, the cosmological bound allows a mass splitting up to 8%. In Fig.15 we plot the allowed regions at $\tan\beta = 34$ (a) and 42 (b). We notice in all cases that slepton coannihilations constrain $m_{\tilde{\chi}}$ to less than approx. 0.5 TeV, while in the case of the sbottom the bound is three times higher.

Remarkably, we see in Fig.14 and 15 that the 2- σ bound on a coming from de-

decay data is always fulfilled in the parameter space regions allowed by the other cosmological constraints.

As regards non-zero values for A_0 , we draw in the present case the same conclusions as in the preceding section (see Fig.13): the type of phenomenological constraint giving the lower bound on $m_{\tilde{\chi}}^0$ in general changes, but the lowest value of $m_{\tilde{\chi}}^0$ is determined by the $A_0 = 0$ case.

The coannihilation pattern is in this case by far more complicated than in the sbottom case. We show in Fig.16 a typical situation for the (percent) contributions of the possible coannihilating initial sparticles, and a detail of the most relevant final states, taken at $m_{\tilde{\tau}} \approx m_{\tilde{\chi}}^0$ and $\tan \beta = 38$. This pattern is however rather dependent on the $\tan \beta$ value and on the relative mass splitting. The case of stau-tau sneutrino coannihilations is further discussed in the Appendix.

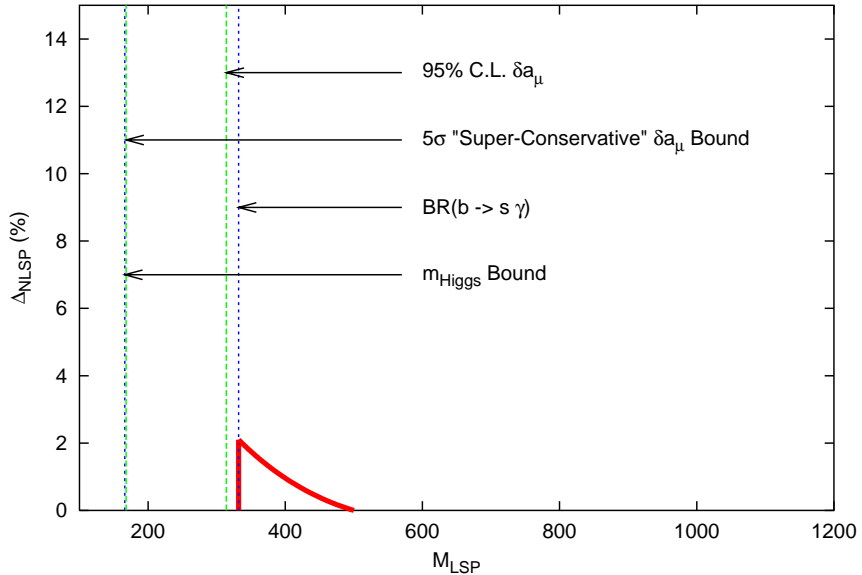


Figure 14: Cosmologically allowed parameter space in the tau Sneutrino-stau coannihilation region, at $K = 0.1$ and $\tan \beta = 38.0$. The scale of the axis, as well as the notation, are the same as in Fig.11.

7 Conclusions

In this paper we studied the cosmological and phenomenological consequences of top-down b-Yukawa Coupling Unification with minimal non-Universal boundary conditions in the sfermion masses, inspired by SU(5) GUT. We showed that the $b > 0$ case is ruled out by the b-quark mass bound. We stress that this result holds also in the particular case of full universality (CMSSM). As for the $b < 0$ case, we pinned down the range of $\tan \beta$ for which b-YU is compatible with the set of all known cosmological constraints, among which the recent results from WMAP. A large parameter space region

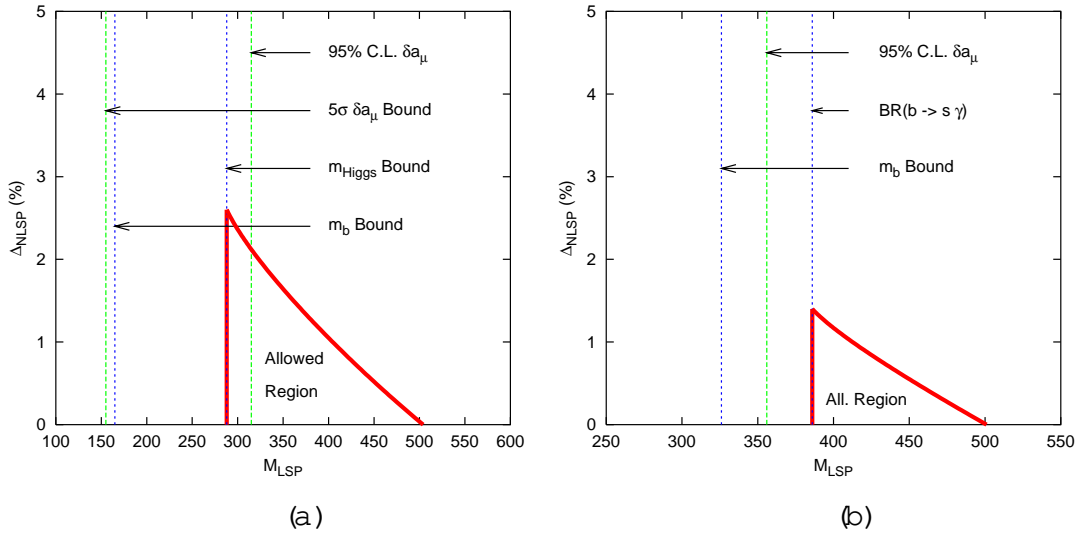


Figure 15: Cosmological allowed parameter space in the tau sneutrino-stau Coannihilation region at $K = 0.1$, $\tan \beta = 34.0$ (a) and $\tan \beta = 42.0$ (b).

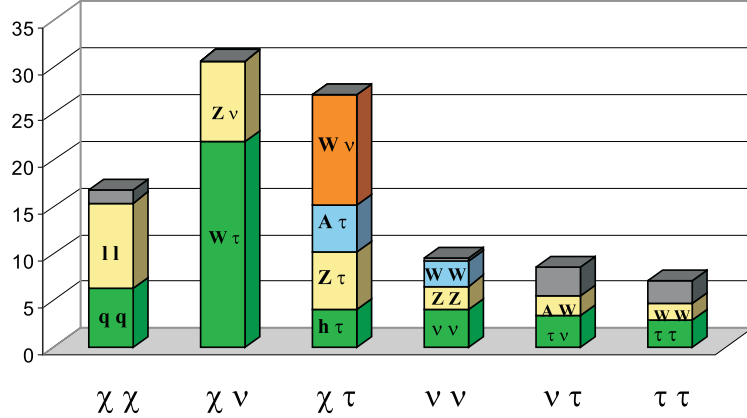


Figure 16: A typical pattern of the relative contribution of coannihilation processes in the tau sneutrino coannihilation region. The plot refers to the case $\tan \beta = 34$, $A_0 = 0$ and $m \sim ' m \sim \tau$. The upper gray part of the columns represents other contributing channels.

is also found to be consistent with the 2- range of a determined from decay data. Further, if one resorts to a super-conservative approach [53] to a , the whole allowed regions discussed would fulfill the resulting bound.

We found that the SUSY spectrum allows for new types of coannihilations, namely neutralino-sbottom and neutralino-tau sneutrino-stau, that we analyzed in detail. We fixed three Benchmark scenarios for the three possible coannihilation patterns, including the CMSSM-like case of neutralino-stau, and we showed for these three cases the behavior of the cosmological and phenomenological constraints as functions of the LSP mass. We

then discussed the cosmologically allowed regions for the two types of new coannihilations at various values of $\tan\beta$, and the main channels contributing to the neutralino relic density suppression. An analytical approximate treatment of these channels is given in the Appendix.

Acknowledgments

I would like to thank S. Bertolini, S. Petcov, P. Ullio and C.E. Yaguna for many useful discussions, comments and for support. I also acknowledge C. Pallis for collaboration during the early stages of this work.

A Neutralino Relic Density Calculation in the presence of Coannihilations

The starting point to compute the neutralino relic density is the generalization of the Boltzmann equation to a set of N coannihilating species [51, 10]

$$\frac{dn}{dt} = -3Hn \langle \sigma v \rangle n^2 n_{eq}^2; \quad (31)$$

where H is the Hubble constant, $n = \sum_{i=1}^N n_i$ is the total number density summed over all coannihilating particles, n_{eq} is the equilibrium number density, which in the Maxwell-Boltzmann approximation, valid in the present cases, reads

$$n_{eq} = \frac{T}{2\pi^2} \sum_{i=1}^N g_i m_i^2 K_2 \left(\frac{m_i}{T}\right) \quad (32)$$

g_i being the internal degrees of freedom of particle i of mass m_i , T the photon temperature and $K_2(x)$ a modified Bessel function. In Eq.(31) $\langle \sigma v \rangle$ is the effective cross section, defined as

$$\langle \sigma v \rangle = \sum_{i,j=1}^N \sigma_{ij} r_i r_j; \quad (33)$$

In its turn, σ_{ij} is the total cross section for the processes involving ij (co-)annihilations, averaged over initial spin and particle-antiparticle states. The coefficients r_i , in the reasonable approximation [10] where the ratio of the number density of species i to the total number density maintains its equilibrium before, during and after freeze out, are defined as

$$r_i = \frac{n_{eq}^i}{n_{eq}} = \frac{g_i (1 + \frac{m_i}{m_{eq}})^{3/2} e^{-\frac{m_i}{T}}}{g_{tot}} \quad (34)$$

where

$$g_{tot} = \sum_{i=1}^N g_i (1 + \frac{m_i}{m_{eq}})^{3/2} e^{-\frac{m_i}{T}}; \quad \frac{m_i}{m_{eq}} = \frac{m_i - m_{eq}}{m_{eq}}; \quad x = \frac{m_{eq}}{T}; \quad (35)$$

From (34) it is apparent that only species which are quasi degenerate in mass with the LSP can effectively contribute to the coannihilation processes, since large mass differences

are exponentially suppressed. Once numerically determined the freeze-out temperature T_F [11], the LSP relic density at the present cosmological time can be evaluated by [10]

$$\sim h^2 \frac{1.07 \cdot 10^9 \text{ GeV}^{-1}}{g_{\text{eff}}^{1/2} M_P x_F^{-1} \hat{v}_e}; \quad (36)$$

where $M_P = 1.22 \cdot 10^{19} \text{ GeV}$ is the Planck scale, $g_{\text{eff}} = 81$ is number of effective degrees of freedom at freeze out, $x_F = m \sim T_F$ and

$$\hat{v}_e = x_F \int_{x_F}^{x_F} h_e v dx; \quad (37)$$

keeps track of the efficiency of post-freeze-out annihilations.

In many cases, one can approximate the themally averaged product of the relative velocity and the cross section of the (co-)annihilating particles through a Taylor expansion

$$v_{ij} = a_{ij} + b_{ij} v^2 \quad (38)$$

This approximation is not accurate near s-channel poles and final-state thresholds, as pointed out in Ref. [10, 12]. In all other cases, and namely in the great part of the ones studied in the present paper (an exception is given in Fig. 5), one can proceed and calculate

$$\hat{v}_e = \sum_{ij} \left(\frac{a_{ij}}{x_{ij}} + \frac{b_{ij}}{x_{ij}} \right) \hat{v}_{ij}; \quad (39)$$

where the sum is extended to all the possible pairs of initial sparticle states, and the coefficients

$$\hat{v}_{ij} = x_F \frac{dx}{x^2} r_i(x) r_j(x); \quad \hat{v}_{ij} = 6x_F \frac{dx}{x^3} r_i(x) r_j(x); \quad (40)$$

We list in Tables 2 – 5 all the possible annihilation and coannihilation processes involving the neutralino, the stau, the sbottom and the tau sneutrino. Only a subset of these reactions effectively contribute to the reduction of the neutralino relic density, as described in Sec. 6.1 and 6.2. In particular, contrary to the case of neutralino annihilation, the largest contributions to (39) arising from coannihilation processes come from the a_{ij} coefficients. In Sec. A 2 we give the analytical form of the a_{ij} for the "new" coannihilations which arise in the present context of mNsum. Namely, we study the most relevant processes in the cases of sbottom-neutralino, sbottom-sbottom and stau-tau sneutrino coannihilations. A numerical check of the formula given in Sec. A 2, consisting in a comparison between the computation outlined in this Appendix and the numerical result given by micrOMEGAs confirms the expected validity of this approximate treatment to a satisfactory extent, in the regimes not affected by the A-pole effects.

A .1 The Coannihilation processes

We report in Tables 2 – 5 the complete list of all (Co-)annihilation processes involving the lightest neutralino, sbottom and stau as well as the tau sneutrino. For a given couple of initial sparticles we list both all the possible final states and the tree level channels relative to any final state. $c m$ eans 4-particles contact interaction, while $s(X)$; $t(X)$ and $u(X)$ mean an s, t or u channel where X is the exchanged (s)particle. d and u indicate respectively the down and up-type quarks, while l and \bar{l} the charged leptons and the neutrinos of any family, where not differently specified. f stands for a generic fermion (quark or lepton).

Initial State	Final States	Tree Level Channels
$\sim \sim$	$h h, h H, H H, A A, Z Z, A Z,$ $h H] A, h H] Z$ $W^+ W^-, H^+ H^-$ $W^- H$ $f \bar{f}$	$s(h), s(H), t(\sim_i^0), u(\sim_i^0)$ $s(A), s(Z), t(\sim_i^0), u(\sim_i^0)$ $s(h), s(H), s(Z), t(\sim_j^0), u(\sim_j^0)$ $s(h), s(H), s(A), t(\sim_j^0), u(\sim_j^0)$ $s(h), s(H), s(A), s(Z), t(f), u(f)$
$\sim \tilde{b}$	$b h H], b Z$ $b A$ $b^-, b g$ $t H^-, t W^-$	$s(b), t(\tilde{b}_{1,2}), u(\sim_i^0)$ $s(b), t(\tilde{b}_2), u(\sim_i^0)$ $s(b), t(\tilde{b}_1)$ $s(b), t(\tilde{b}_{1,2}), u(\sim_j^0)$
$\sim \tilde{\tau}_1$	$h H], Z$ A H^-, W^-	$s(\), t(\tilde{\tau}_2), u(\sim_i^0)$ $s(\), t(\tilde{\tau}), u(\sim_i^0)$ $s(\), t(\tilde{\tau})$ $s(\), t(\sim), u(\sim_j^0)$
$\sim \sim$	$h H], Z$ A H^+, W^+	$s(\), t(\sim), u(\sim_i^0)$ $u(\sim_i^0)$ $s(\), t(\sim_{1,2}), u(\sim_j^0)$

Table 2: Neutralino Annihilations and Coannihilation with sbottom, stau and sneutrino.

Initial State	Final States	Tree Level Channels
$\tilde{b}_1 \tilde{b}_1$	$b b$	$t(\tilde{b}_1^0), u(\tilde{b}_1^0), t(g), u(g)$
$\tilde{b}_1 \tilde{b}_1$	$h h, h H, H H, Z Z$	$s(h), s(H), t(\tilde{b}_{1,2}), u(\tilde{b}_{1,2}), c$
	$A A$	$s(h), s(H), t(\tilde{b}_2), u(\tilde{b}_2), c$
	$Z A$	$s(h), s(H), t(\tilde{b}_2), u(\tilde{b}_2)$
	$A h H]$	$s(Z), t(\tilde{b}_2), u(\tilde{b}_2)$
	$Z h H]$	$s(Z), t(\tilde{b}_{1,2}), u(\tilde{b}_{1,2})$
	$W^+ W^-, H^+ H^-$	$s(h), s(H), s(Z), t(\tilde{b}_{1,2}), c, s(\)$
	$W^- H$	$s(h), s(H), t(\tilde{b}_{1,2})$
	$t \bar{t}, u \bar{u}$	$s(h), s(H), s(Z), s(\), s(g), t(\tilde{b}_j), t(g)$
	$b \bar{b}$	$s(h), s(H), s(Z), s(\), s(g), t(\tilde{b}_j), t(g)$
	$d \bar{d}$	$s(h), s(H), s(Z), s(\), s(g)$
	$l \bar{l}$	$s(h), s(H), s(Z), s(\)$
	$-$	$s(Z)$
	$, Z, g, Z g$	$t(\tilde{b}_1), u(\tilde{b}_1), c$
	$h H], g h H]$	$t(\tilde{b}_1), u(\tilde{b}_1)$
	$g g$	$s(g), t(\tilde{b}_1), u(\tilde{b}_1), c$
$\tilde{b}_1 \tilde{\chi}_1^0$	b	$t(\tilde{\chi}_1^0)$
$\tilde{b}_1 \tilde{\chi}_1^0$	b^-	$t(\tilde{\chi}_1^0)$
	t^-	$t(\tilde{\chi}_j^0)$
$\tilde{b}_1 \sim$	b	$t(\tilde{\chi}_1^0)$
	t	$t(\tilde{\chi}_j^0)$
$\tilde{b}_1 \sim$	b^-	$t(\tilde{\chi}_1^0)$

Table 3: Sbottom Annihilations and Coannihilations with stau and sneutrino.

Initial State	Final States	Tree Level Channels
$\tilde{\chi}_1^0 \tilde{\chi}_1^0$		$t(\tilde{\chi}_1^0), u(\tilde{\chi}_1^0)$
$\tilde{\chi}_1^0 \tilde{\chi}_1^0$	$h h, h H, H H, Z Z$ $A A$ $A Z$ $A h H]$ $Z h H]$ $W^+ W^-, H^+ H^-$ $W^- H$ $u \bar{u}, d \bar{d}, l \bar{l}$ $-$ $-$ $-$ $, Z$ $h H]$	$s(h), s(H), t(\tilde{\chi}_1^0), u(\tilde{\chi}_1^0), c$ $s(h), s(H), t(\tilde{\chi}_1^0), u(\tilde{\chi}_1^0), c$ $s(h), s(H), t(\tilde{\chi}_1^0), u(\tilde{\chi}_1^0)$ $s(Z), t(\tilde{\chi}_1^0), u(\tilde{\chi}_1^0)$ $s(Z), t(\tilde{\chi}_1^0), u(\tilde{\chi}_1^0)$ $s(h), s(H), s(Z), u(\tilde{\chi}_1^0), c, s(\tilde{\chi}_1^0)$ $s(h), s(H), u(\tilde{\chi}_1^0)$ $s(h), s(H), s(Z), t(\tilde{\chi}_1^0), s(\tilde{\chi}_1^0)$ $s(Z), t(\tilde{\chi}_1^0)$ $s(Z)$ $c, t(\tilde{\chi}_1^0), u(\tilde{\chi}_1^0)$ $t(\tilde{\chi}_1^0), u(\tilde{\chi}_1^0)$
$\tilde{\chi}_1^0 \tilde{\chi}_1^0$		$t(\tilde{\chi}_1^0), u(\tilde{\chi}_1^0)$
$\tilde{\chi}_1^0 \tilde{\chi}_1^0$	$\bar{u} d, \bar{l} l$ $-$ $Z W$ W $Z H$ H $W^- h, W^- H$ $W^- A$ $H^- h, H^- H$ $H^- A$	$s(H), s(W)$ $s(W), s(H), t(\tilde{\chi}_1^0)$ $s(W), u(\tilde{\chi}_1^0), t(\tilde{\chi}_1^0), c$ $s(W), u(\tilde{\chi}_1^0), c$ $s(H), u(\tilde{\chi}_1^0), t(\tilde{\chi}_1^0)$ $s(H), u(\tilde{\chi}_1^0)$ $s(H), s(W), u(\tilde{\chi}_1^0), t(\tilde{\chi}_1^0)$ $s(H), u(\tilde{\chi}_1^0)$ $s(H), s(W), u(\tilde{\chi}_1^0), t(\tilde{\chi}_1^0), c$ $s(W), u(\tilde{\chi}_1^0), c$

Table 4: Stau Annihilations and Coannihilations with sneutrino.

Initial State	Final States	Tree Level Channels
$\tilde{\chi}_1^0 \tilde{\chi}_1^0$		$t(\tilde{\chi}_1^0), u(\tilde{\chi}_1^0)$
$\tilde{\chi}_1^0 \tilde{\chi}_1^0$	$h h, h H, H H, Z Z$	$s(h), s(H), t(\tilde{\chi}_1^0), u(\tilde{\chi}_1^0), c$
	$A A$	$s(h), s(H), c$
	$Z A$	$s(h), s(H)$
	$Z h H$	$s(Z), t(\tilde{\chi}_1^0), u(\tilde{\chi}_1^0)$
	$W^+ W^-, H^+ H^-$	$s(h), s(H), s(Z), t(\tilde{\chi}_1^0), c$
	$W^+ H^-$	$s(h), s(H), t(\tilde{\chi}_1^0)$
	$u \bar{u}, d \bar{d}, l \bar{l}$	$s(h), s(H), s(Z)$
	—	$s(h), s(H), s(Z), t(\tilde{\chi}_1^0)$
	—	$s(Z), t(\tilde{\chi}_1^0)$
	$A h H$	$s(Z)$

Table 5: Sneutrino Annihilations.

A.2 Relevant Approximate Formul for the Relic Density Calculation in the Coannihilation Regions

The coefficients for the pair annihilation of neutralinos can be readily and completely derived from Ref [67], while those concerning the stau annihilations and coannihilations can be calculated from the formul of Ref. [68] and [13, 37]. As regards the tau sneutrino (Co-)annihilations, the relative coefficients can be readily derived from those of the stau via suitable replacements in the couplings (e.g. $g_{\tilde{\chi}_1^0 h} \rightarrow g_{\tilde{\chi}_1^0 h}$ etc.), in the masses of the (s-)particles (e.g. $m_{\tilde{\chi}_1^0} \rightarrow m_{\tilde{\chi}_1^0}$) and setting the mixing angle between the stau mass eigenstates to zero. We do not give any explicit formula for the sbottom-stau and the sbottom-sneutrino coannihilations since even in the transition regions where $m_{\tilde{b}} \approx m_{\tilde{\chi}_1^0} \approx m_{\tilde{\tau}}$ these processes do not give any sizeable contribution to the neutralino relic density suppression (namely, their total contribution is always less than 0.5%). Therefore we are left with the "new" (co-)annihilation processes involving respectively neutralino-sbottom, sbottom-sbottom and stau-tau sneutrino.

We give here the explicit formul for the dominant processes, as discussed in Sec.6.1 and 6.2. In the kinematic part of the coefficients we neglect the mass of the Standard Model Particles up to the b-quark included. Since the mass of the SM particles m_{SM} appear there as $m_{SM}^2 \approx m_{SUSY}^2$, the corrections are in fact always negligible. On the other hand, we keep trace of both m_b and $m_{\tilde{b}}$ if the couplings or the whole amplitudes are proportional to them, as it is the case in some of the considered processes. Moreover, in the processes involving the sbottom we followed the approximations of Ref. [15] neglecting the term s in $m_{\tilde{b}}$ and $m_{\tilde{\tau}}$. Bar over a mass means that the mass is divided by the sum of the masses of the incoming sparticles. S stands for the three neutral physical Higgs h ,

H and A , and m_s for the respective masses, $s_x = \sin x$, $c_x = \cos x$ and for the other symbols we follow the notation of Ref. [3].

A 2.1 Couplings

g Symbol	Expression
$g_{b_1 b_{\sim i}}^L$	$\frac{g_2}{2} c_b N_{i2} \frac{\tan w}{6} N_{i1} + s_b \frac{m_b N_{i3}}{m_w \cos}$
$g_{b_1 b_{\sim i}}^R$	$\frac{g_2}{2} c_b \frac{m_b N_{i3}}{m_w \cos} + \frac{2}{3} s_b \tan w N_{i1} \text{sign}(m_{\sim i}^0)$
$g_{b_1 b_1 g} = g_{b_1 g} = g_{ggg}$	g_s
$g_{b_1 b_1 g}^L$	$\frac{p}{2} g_s s_b$
$g_{b_1 b_1 g}^R$	$\frac{p}{2} g_s c_b$
$g_{b_1 b_{\sim i}}^L$	$\frac{1}{2} g_{b_1 b_{\sim i}}^L + g_{b_1 b_{\sim i}}^R$
$g_{b_1 b_{\sim i}}$	$\frac{1}{2} g_{b_1 b_{\sim i}}^L g_{b_1 b_{\sim i}}^R$
$g_{b_1 b_1 gg}$	g_s^2
$g_{h H \gamma_1 \gamma_1}$	$\frac{g_2}{2 c_w} m_z s + [c_+] (1 - 2 s_w^2) s_{\sim}^2 + 2 s_w^2 c_{\sim}^2 + \frac{g_2 m_h}{M_w c} m_s [c] + s_{\sim} c_{\sim} A_s [c] + c [s]$
$g_{A \gamma_1 \gamma_1}$	0
$g_{W \sim \gamma_1}$	$\frac{g_2 s_{\sim}}{2}$
$g_{W \sim \gamma_2}$	$\frac{g_2 c_{\sim}}{2}$
$g_{H^+ h H \gamma_W}$	$\frac{g_2}{2} c [s]$
$g_{H^+ A W}$	$\frac{g_2}{2}$
$g_{H^+ \sim \gamma_1}$	$\frac{g_2 M_w s_{\sim}}{2} s_2$

Table 6: Relevant couplings used in the formul of Sec A 2.2 (I)

g Symbol	Expression
$g_{h H \gamma W + W}$	$g_2 M_W s_- [c_+]$
$g_{A W + W}$	0
$g_{h H \gamma_1 \gamma_2}$	$\frac{g_2}{2c_W} m_z s_- + [c_+](1 - 4s_W^2) s_- c_-$ $+ g_2 m_- (c_-^2 - s_-^2) \frac{A_- s_- [c_+] + c_- [s_-]}{2M_W c_-}$
$g_{A \gamma_1 \gamma_2}$	$g_2 m_- \frac{A_- \tan_- +}{2M_W}$
$g_W z \sim \gamma_1$	$p_- \frac{g_2^2 s_W^2}{2c_W} s_-$
$g_W w z$	$g_2 c_W$
$g_W tb$	$p_- \frac{g_2}{2}$
$g_{H^+ tb}^L$	$p_- \frac{g_2}{2M_W} (m_t \cot_-)$
$g_{H^+ tb}^R$	$p_- \frac{g_2}{2M_W} (m_b \tan_-)$
$g_{\gamma_1 \gamma_i^0}^L$	$s_- p_- \frac{g_2}{2M_W} \frac{N_{i3} m_-}{c_-} + c_- \frac{p_-}{c_W} \frac{2g_2}{s_W^2} s_W^2 N_{i2}^0 - p_- \frac{2g_1 c_W}{2g_1 c_W} N_{i1}^0$!
$g_{\gamma_1 \gamma_i^0}^R$	$s_- p_- \frac{g_2}{2g_1 c_W} N_{i1}^0 + \frac{g_2}{c_W} \frac{1}{2} s_W^2 N_{i2}^0 - c_- p_- \frac{g_2}{2M_W} \frac{N_{i3} m_-}{c_-}$
$g_{\gamma_i^0 \gamma_i^0}^L$	0
$g_{\gamma_i^0 \gamma_i^0}^R$	$p_- \frac{g_2}{2M_W} N_{i2}^0$
$g_{\gamma_1 \gamma_j^0}^L$	$p_- \frac{g_2}{2M_W} \frac{U_{j2} m_-}{c_-} c_-$
$g_{\gamma_1 \gamma_j^0}^R$	$g_2 U_{j1} s_-$
$g_{\gamma_i^0 \gamma_j^0}^L$	$p_- \frac{g_2}{2M_W} \frac{U_{j2} m_-}{c_-}$
$g_{\gamma_i^0 \gamma_j^0}^R$	$g_2 V_{j1}$

Table 7: Relevant couplings used in the formul of Sec A.2.2 (II)

A.2.2 ~ \tilde{b}_1 Coannihilations

$$\begin{aligned}
 & \frac{1}{24 m_{\tilde{b}_1}^2} g_{\tilde{b}_1 b \sim_1}^L + g_{\tilde{b}_1 b \sim_1}^R h g_{\tilde{b}_1 \tilde{b}_1 g}^2 (m_{\sim_1}^0 - m_{\tilde{b}_1}) + g_{b \tilde{b}_1 g}^2 m_{\tilde{b}_1} \\
 & - 4 g_{b \tilde{b}_1 g} g_{\tilde{b}_1 \tilde{b}_1 g} \left(g_{\tilde{b}_1 b \sim_1}^L \right)^2 + \left(g_{\tilde{b}_1 b \sim_1}^R \right)^2 (m_{\sim_1}^0 - m_{\tilde{b}_1})
 \end{aligned}$$

A.2.3 \tilde{b}_1 Annihilations

$$\begin{aligned}
 & \frac{g_{\tilde{b}_1 b \tilde{g}}^L \left(g_{\tilde{b}_1 b \tilde{g}}^R \right)^2 + g_{\tilde{b}_1 b \tilde{g}}^R \left(g_{\tilde{b}_1 b \tilde{g}}^L \right)^2}{54 m_{\tilde{g}}^2 + m_{\tilde{b}_1}^2} \\
 & + X^4 \left(\sum_{i,j=1}^2 \frac{g_{\tilde{b}_1 b \sim_i}^2 + g_{\tilde{b}_1 b \sim_i}^2 g_{\tilde{b}_1 b \sim_j}^2 + g_{\tilde{b}_1 b \sim_j}^2}{m_{\sim_i}^2 + m_{\tilde{b}_1}^2} \right. \\
 & \left. + \frac{4 m_{\sim_i} m_{\sim_j} g_{\tilde{b}_1 b \sim_i} g_{\tilde{b}_1 b \sim_i} g_{\tilde{b}_1 b \sim_j} g_{\tilde{b}_1 b \sim_j}}{4 m_{\sim_i}^2 + m_{\tilde{b}_1}^2 m_{\sim_j}^2 + m_{\tilde{b}_1}^2} \right) \\
 & + \frac{81 g_{ggg}^2 g_{\tilde{b}_1 \tilde{b}_1 g}^2 + 56 g_{\tilde{b}_1 \tilde{b}_1 gg} 2 g_{\tilde{b}_1 \tilde{b}_1 gg} g_{\tilde{b}_1 \tilde{b}_1 g}}{1728 m_{\tilde{b}_1}^2}
 \end{aligned}$$

$$\begin{aligned}
 & \frac{1}{128} \frac{M_W + m_S^2}{M_W^2 m_\sim m_{\tilde{\chi}_1}} \frac{1}{m_\sim m_{\tilde{\chi}_1}} \frac{m_S^2}{m_\sim m_{\tilde{\chi}_1}} \stackrel{3=2}{\#} \\
 & + \frac{2 g_{H^+ SW}}{1 m_H^2} \frac{g_{H^+ \sim \tilde{\chi}_1} m_\sim}{m_\sim m_{\tilde{\chi}_1}} + \frac{g_{W \sim \tilde{\chi}_1} g_{SW^+ W}}{M_W^2 1 M_W^2} \frac{(m_\sim - m_{\tilde{\chi}_1})^2}{(m_\sim - m_{\tilde{\chi}_1})^2} \stackrel{\#_2}{\#} \\
 & + \frac{2 g_{S \tilde{\chi}_1 \tilde{\chi}_2} g_{W \sim \tilde{\chi}_2} m_\sim}{m_\sim m_S^2 m_\sim^2 m_{\tilde{\chi}_1} m_\sim (m_{\tilde{\chi}_2}^2 + m_{\tilde{\chi}_1}^2)} \frac{m_{\tilde{\chi}_1}}{m_{\tilde{\chi}_1} (m_{\tilde{\chi}_2}^2 - M_W^2)} \stackrel{\#_2}{\#}
 \end{aligned}$$

$$\begin{aligned}
 & \frac{1}{32} \frac{M_W + M_Z^2}{m_\sim m_{\tilde{\chi}_2}} \frac{1}{M_W} \frac{M_Z^2}{m_\sim m_{\tilde{\chi}_2}} \stackrel{1=2}{\#} \\
 & \frac{M_Z^2 + M_Z^2}{2 M_Z M_W} \frac{1}{m_\sim^2} \stackrel{\#}{\#} \\
 & 7 g_W^2 z_{\sim \tilde{\chi}_1} + 7 g_W^2 \sim \tilde{\chi}_1 g_W^2 w_Z \frac{1}{m_W^2} \stackrel{\#}{\#} \\
 & + 4 g_W z_{\sim \tilde{\chi}_1} g_W \sim \tilde{\chi}_1 g_W w_Z \frac{1}{m_W^2} \stackrel{\#}{\#}
 \end{aligned}$$

$$\begin{aligned}
 & \frac{1}{16} \frac{m_t^2}{m_\sim m_{\tilde{\chi}_1}} \frac{g_W^2 \sim \tilde{\chi}_1 g_W^2 tb}{m_b m_t} \frac{m_b m_t}{M_W^4} \stackrel{\#}{\#} \\
 & + \frac{g_H^2 \sim \tilde{\chi}_1}{1 m_H^2} \frac{h}{2} \frac{g_{H^+ tb}^L}{g_{H^+ tb}^L} \frac{2}{m_b m_t} + \frac{g_{H^+ tb}^R}{g_{H^+ tb}^L} \frac{2}{m_b m_t} \frac{1}{m_t^2} \stackrel{\#}{\#} \\
 & + \frac{g_{H^+ \sim \tilde{\chi}_1} g_W \sim \tilde{\chi}_1 g_W tb}{M_W^2 1 m_H^2} \frac{g_{H^+ tb}^L m_t}{m_t^2} \frac{1}{m_t^2} \frac{g_{H^+ tb}^R m_b}{m_b^2} \frac{1}{1 + m_t^2}
 \end{aligned}$$

"
#

m^2

$($

X^4

$m^2 \text{ Re } g_{\gamma_1}^L \gamma_i^0 g_{\gamma_1}^L \gamma_k^0 g_{\gamma_1}^R \gamma_i^0 g_{\gamma_1}^R \gamma_k^0$

$\frac{32 m \sim m_{\gamma_1}}{i \neq k = 1}$

$-$

$m_{\gamma_i^0}^2 + m \sim m_{\gamma_1}$

$m_{\gamma_k^0}^2 + m \sim m_{\gamma_1}$

"
#

X^4

$m^2 \text{ Re } g_{\gamma_1}^L \gamma_i^0 g_{\gamma_1}^L \gamma_k^0 g_{\gamma_1}^R \gamma_i^0 g_{\gamma_1}^R \gamma_k^0$

$+ \frac{i \neq k = 1}{m_{\gamma_i^0}^2 + m \sim m_{\gamma_1} \quad m_{\gamma_k^0}^2 + m \sim m_{\gamma_1}}$

"
#

X^2

$m_{\gamma_1}^2 \text{ Re } g_{\gamma_1}^L \gamma_j \gamma_1 g_{\gamma_1}^R \gamma_j \gamma_1 g_{\gamma_1}^R \gamma_j \gamma_1$

$+ \frac{j \neq 1}{m_{\gamma_j}^2 + m \sim m_{\gamma_1} \quad m_{\gamma_1}^2 + m \sim m_{\gamma_1}}$

"
#

X^2

$m_{\gamma_1}^2 \text{ Re } g_{\gamma_1}^L \gamma_j \gamma_1 g_{\gamma_1}^R \gamma_j \gamma_1 g_{\gamma_1}^R \gamma_j \gamma_1$

$+ \frac{j \neq 1}{m_{\gamma_j}^2 + m \sim m_{\gamma_1} \quad m_{\gamma_1}^2 + m \sim m_{\gamma_1}}$

"
#

$X^4 \quad X^2 \quad m_{\gamma_1} m \sim \text{Re } g_{\gamma_1}^L \gamma_j g_{\gamma_1}^L \gamma_i^0 g_{\gamma_1}^R \gamma_i^0 g_{\gamma_1}^R \gamma_j$

$\frac{i=1 \quad j=1}{m_{\gamma_i^0}^2 + m \sim m_{\gamma_1} \quad m_{\gamma_j}^2 + m \sim m_{\gamma_1}}$

"
#

$X^4 \quad X^2 \quad m_{\gamma_1} m \sim \text{Re } g_{\gamma_1}^L \gamma_i^0 g_{\gamma_1}^L \gamma_j g_{\gamma_1}^R \gamma_j g_{\gamma_1}^R \gamma_i^0$

$\frac{i=1 \quad j=1}{m_{\gamma_i^0}^2 + m \sim m_{\gamma_1} \quad m_{\gamma_j}^2 + m \sim m_{\gamma_1}}$

"
#

References

- [1] For a review on Grand Unified Theories see e.g. P. Langacker, *Phys. Rep.* 72 (1981) 185.
- [2] For a review on SUSY GUTs see e.g. W. de Boer, *Prog. Part. Nucl. Phys.* 33 (1994) 201.
- [3] H. E. Haber and G. L. Kane, *Phys. Rep.* 117 (1985) 76;
J. F. Gunion and H. E. Haber, *Nucl. Phys. B* 272 (1986) 1.
- [4] A. Chamseddine, R. Arnowitt and P. Nath, *Phys. Rev. Lett.* 49 (1982) 970;
R. Barbieri, S. Ferrara and C. Savoy, *Phys. Lett. B* 119 (1982) 343;
L. J. Hall, J. Lykken and S. Weinberg, *Phys. Rev. D* 27 (1983) 2359.
- [5] S. Profumo, Talk given at the XXXVIIth Rencontres de Moriond on Electroweak Interactions and Unified Theories, March 15th to 22nd, 2003.
- [6] D. N. Spergel et al., [astro-ph/0302209](#).
- [7] J. Ellis, K. A. Olive, Y. Santoso and V. C. Spanos, [hep-ph/0303043](#).
- [8] H. Baer, C. Balazs, [hep-ph/0303114](#); A. B. Lahanas, D. V. Nanopoulos, [hep-ph/0303130](#)
- [9] P. Salati, [astro-ph/0207396](#).
- [10] K. G. Riess and D. Scolnic, *Phys. Rev. D* 43 (1991) 3191.
- [11] K. G. Riess, M. K. Kowalski and M. S. Turner, *Phys. Rev. D* 41 (1990) 3565.
- [12] P. Gondolo and G. Gelmini, *Nucl. Phys. B* 360 (1991) 145.
- [13] J. Ellis, T. Falk, K. A. Olive and M. Srednicki, *Astropart. Phys.* 13 (2000) 181; *Erratum - ibid.* 15 (2001) 413.
- [14] H. Baer, C. Balazs, A. Belyaev, *JHEP* 0203 (2002) 042.
- [15] J. Ellis, K. A. Olive and Y. Santoso, *Astropart. Phys.* 18 (2003) 395.
- [16] J. Edsjo, M. Schelke, P. Ullio and P. Gondolo, [hep-ph/0301106](#).
- [17] B. A. Nanthnarayan, G. Lazarides and Q. Shafi, *Phys. Rev. D* 44 (1991) 1613 and *Phys. Lett. B* 300 (1993) 245;
G. Anderson et al. *Phys. Rev. D* 47 (1993) 3702 and *Phys. Rev. D* 49 (1994) 3660;
V. Barger, M. Berger and P. Ohmann, *Phys. Rev. D* 49 (1994) 4908;
B. A. Nanthnarayan, Q. Shafi and X. Wang, *Phys. Rev. D* 50 (1994) 5980;
R. Rattazzi and U. Sarid, *Phys. Rev. D* 53 (1996) 1553.
- [18] M. Carena, M. Olechowski, S. Pokorski and C. E. Wagner, *Nucl. Phys. B* 426 (1994) 269.

[19] L.J. Hall, R. Rattazzi and U. Sarid, *Phys. Rev. D* 50 (1994) 7048;
 R. Hemping, *Phys. Rev. D* 49 (1994) 6168.

[20] M.S. Chanowitz, J. Ellis and M.K. Gaillard, *Nucl. Phys. B* 128 (1977) 506;
 A.J. Buras, J. Ellis, M.K. Gaillard and D.V. Nanopoulos, *Nucl. Phys. B* 135 (1978) 66.

[21] M.B. Einhorn and D.R. Jones, *Nucl. Phys. B* 196 (1982) 475;
 L.E. Ibanez and C. Lopez, *Nucl. Phys. B* 233 (1984) 511;
 H. Arason, D. Castano, B. Keszthelyi, S. Mikaelian, E. Piard, P. Ramond and
 B. Wright, *Phys. Rev. Lett.* 67 (1991) 2933;
 A. Giveon, L.J. Hall and U. Sarid, *Phys. Lett. B* 271 (1991) 138;
 S. Kelley, J.L. Lopez and D.V. Nanopoulos, *Phys. Lett. B* 274 (1992) 387.

[22] P. Langacker and N. Polonsky, *Phys. Rev. D* 49 (1994) 1454;
 W.A. Bardeen, M. Carena, S. Pokorski and C.E. Wagner, *Phys. Lett. B* 320 (1994) 110.

[23] M. Carena, S. Pokorski and C.E. Wagner, *Nucl. Phys. B* 406 (1993) 59.

[24] N. Polonsky, *Phys. Rev. D* 54 (1996) 4537.

[25] S. Komine and M. Yamaguchi, *Phys. Rev. D* 65 (2002) 075013;
 U. Chattopadhyay and P. Nath, *Phys. Rev. D* 65 (2002) 075009.

[26] W. de Boer, M. Huber, A.V. Gladyshev, D.I. Kazakov, *Eur. Phys. J. C* 20 (2001) 689.

[27] U. Chattopadhyay, A. Corsetti and P. Nath, *Phys. Rev. D* 66 (2002) 035003.

[28] S.M. Barr and I. Dorsner, *Phys. Lett. B* 556 (2003) 185.

[29] B. Bajc, G. Senjanovic and F. Vissani, *Phys. Rev. Lett.* 90 (2003) 051802.

[30] A. Masiero, S.K. Vempati and O. Vives, *Nucl. Phys. B* 649 (2003) 189.

[31] M. Drees, [hep-ph/9611409](#);
 S.M. Martin, in *Perspectives in Supersymmetry*, G. Kane (Editor), [hep-ph/9709356](#);
 S. Dawson in *Proc. TASI 97*, J. Bagger (Editor), [hep-ph/9712464](#).

[32] S. Dimopoulos and D. Sutter, *Nucl. Phys. B* 452 (1995) 496; H. Haber, *Nucl. Phys. Proc. Suppl.* 62 (1998) 469

[33] A. Birkedal Hansen, B.D. Nelson, [hep-ph/0211071](#);
 S.I. Blityukov, N.V. Krasnikov, *Phys. Atom. Nucl.* 65 (2002) 1341;
 H. Baer, C. Balazs, A. Belyaev, R. Dermisek, A. Ma and A. Mustafayev, *JHEP* 0205 (2002) 061;
 N. Chamoun, C.S. Huang, C. Liu and X.H. Wu, *Nucl. Phys. B* 624 (2002) 81.

[34] V. Bertin, E. Nezri and J. Orob, *JHEP* 0302 (2003) 046.

[35] S.K. Soni and H.A. Weldon Phys. Lett. B 126 (1983) 215.

[36] A. Datta, M. Guchait, N. Panua, Phys. Lett. B 395 (1997) 54;
 A. Datta, A. Datta, M.K. Parida, Phys. Lett. B 431 (1998) 347;
 E. Acoomando, R. Amowitt, B. Dutta and Y. Santoso, Nucl. Phys. B 585 (2000) 124;
 S. Codoban, M. Jurcisin and D. Kazakov, Phys. Lett. B 477 (2000) 223. H. Baer,
 C. Balazs, S. Hesselbach, J.K. Mizukoshi and X. Tata, Phys. Rev. D 63 (2001) 095008;

[37] J. Ellis, T. Falk, K.A. Olive and Y. Santoso, Nucl. Phys. B 652 (2003) 259.

[38] H. Baer, M. Diaz, P. Quintana and X. Tata, JHEP 0004 (2000) 016.

[39] J. Ellis, A. Ferstl, K.A. Olive and Y. Santoso, hep-ph/0302032.

[40] S. Bertolini, F. Borzumati, A. Masiero, G. Ridol, Nucl. Phys. B 353 (1991) 591.

[41] D.M. Pierce, J.A. Bagger, K.T. Matchev and R.J. Zhang, Nucl. Phys. B 491 (1997) 3.

[42] G. Belanger, F. Boudjema, A. Pukhov and A. Semenov, Comput. Phys. Commun. 149 (2002) 103; <http://wwwlapp.in2p3.fr/lapth/micromegas/>

[43] P. Gondolo, J. Edsjo, L. Bergstrom, P. Ullio and T. Baltz, in York 2000, The identification of dark matter, 318, astro-ph/0012234; <http://www.physto.se/edsjo/darksusy>.

[44] S. Heinemeyer, W. Hollik and G. Weiglein, hep-ph/0002213.

[45] G. Belanger, F. Boudjema, A. Pukhov and A. Semenov, hep-ph/0210327.

[46] A. L. Kagan and M. Neubert, Eur. Phys. J. C 7 (1999) 5;
 P. Gambino and M. Misiak, Nucl. Phys. B 611 (2001) 338.

[47] M. Ciuchini, G. Degrassi, P. Gambino and G. Giudice, Nucl. Phys. B 527 (1998) 21;
 G. Degrassi, P. Gambino and G.F. Giudice, JHEP 0012 (2000) 009.

[48] S.P. Martin, J.D. Wells, Phys. Rev. D 64 (2001) 035003.

[49] J. Ellis, T. Falk, K.A. Olive, Phys. Lett. B 444 (1998) 367.

[50] A.B. Lahanas, D.V. Nanopoulos, V.C. Spanos, Phys. Rev. D 62 (2000) 023515.

[51] P. Binetruy, G. Giardino and P. Salati, Nucl. Phys. B 237 (1984) 285.

[52] J. Richardson, M. Spiro and J. Lloyd-Owen, Phys. Rep. 151 (1987) 239;
 T.K. Hemmick et al., Phys. Rev. D 41 (1990) 2074;
 T. Yanagata, Y. Takamori, and H. Utsunomiya, Phys. Rev. D 47 (1993) 1231;
 P.F. Smith, Contemp. Phys. 29 (1998) 159.

[53] S.P. Martin and J.D. Wells, Phys. Rev. D 67 (2003) 015002.

[54] See e.g. M. Kamionkowski, K. Griest, G. Jungman and B. Sadoulet, Phys. Rev. Lett. 74 (1995) 5174; L. Bergstrom, J. Edsjo and P. Gondolo, Phys. Rev. D 58 (1998) 103519.

[55] V. Barger, C.E.M. Wagner, et al, hep-ph/0003154.

[56] K. Hagiwara et al, Phys. Rev. D 66 (2002) 010001; C.T. Sachrajda, Nucl. Instrum. Meth. A 462 (2001) 23.

[57] H. Baer, J. Fernandez, K. Melnikov, X. Tata, Phys. Rev. D 66 (2002) 074007.

[58] M. Carena, D. Garcia, U. Nierste, C.E.M. Wagner, Nucl. Phys. B 577 (2000) 88.

[59] T. Blazek, R. Dermisek, S. Raby, Phys. Rev. Lett. 88 (2002) 111804; Phys. Rev. D 65 (2002) 115004.

[60] R. Barate et al. (ALEPH Collaboration), Phys. Lett. B 429 (1998) 169; K. Abe et al. (BELLE Collaboration), Phys. Lett. B 511 (2001) 151; S. Chen et al. (CLEO Collaboration), Phys. Rev. Lett. 87 (2001) 251807.

[61] F.M. Borzumati, M. Olechowski and S. Pokorski, Phys. Lett. B 349 (1995) 311.

[62] S. Bertolini, F. Borzumati, A. Masiero and G. Ridol, Nucl. Phys. B 353 (1991) 591; R. Barbieri and G.F. Giudice, Phys. Lett. B 309 (1993) 86.

[63] ALEPH, DELPHI, L3 and OPAL Collaborations, The LEP Higgs working Group for Higgs Boson Searches, hep-ex/0107029, LHWG Note/2001-03, <http://lephiggs.web.cern.ch/LEPHIGGS/www/Welcome.html>.

[64] Particle Data Group Collaboration, D.E. Groom et.al, Review of particle physics, Eur. Phys. J. C 15 (2000) 1.

[65] K. Hagiwara, A.D. Martin, D. Nomura and T. Teubner, Phys. Lett. B 557 (2003) 69; M. Davier, S. Eidelman, A. Hocker and Z. Zhang hep-ph/0208177.

[66] A. Nyeler, Talk given at the XXXVIIIth Rencontres de Moriond on Electroweak Interactions and Unified Theories, March 15th to 22nd, 2003.

[67] T. Nishi, L. Roszkowski and R.R. de Austri, JHEP 0203 (2002) 031.

[68] T. Nishi, L. Roszkowski and R.R. de Austri, JHEP 0207 (2002) 024.